

Supporting Information

**Rapid and simple preparation of remarkably stable binary
nanoparticle planet–satellite assemblies**

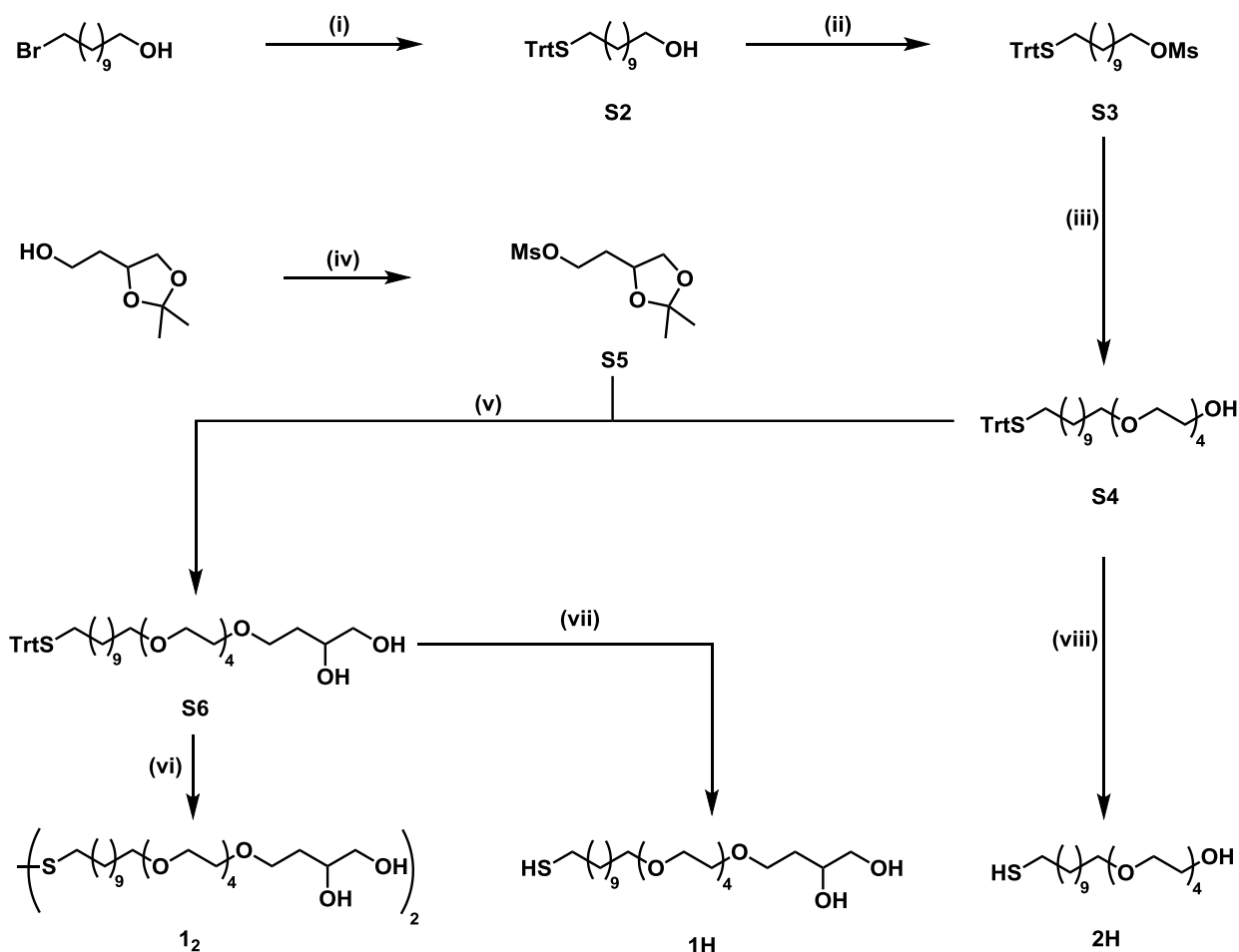
Stefan Borsley, Sarah Flook and Euan R. Kay

1. General experimental procedures	2
2. Synthesis of organic compounds	3
3. Nanoparticle synthesis and characterization.....	10
3.1 AuNP-1	10
3.2 AuNP-2	12
3.4 30 nm Citrate-stabilized NPs.....	14
3.5 Mixed shape citrate-stabilized NPs.....	16
3.6 40 nm Commercial citrate stabilized NPs: Characterization.....	18
3.7 150 nm Commercial citrate stabilized NPs: Characterization.....	19
4. Determination of nanoparticle concentrations	21
5. Planet–satellite preparation and purification.....	23
5.1 Synthetic procedure.....	23
5.2 Determining the optimum mixing ratio	23
5.3 Planet–satellite purification.....	25
5.4 Estimation of planet coverage from TEM imaging	26
5.5 Self-assembly control experiments.....	27
6. Planet–satellite stability studies	28
6.1 Stability to increased temperature	28
6.2 Drying and redispersion of planet–satellite assemblies	29
6.3 Stability to increasing ionic strength.....	31
6.4 Stability to pH.....	32
7. Scope of planet NPs	33
7.1 Varying planet NP size.....	33
7.2 Varying planet NP shape.....	34
8. Varying Satellite NP Size: Preliminary Studies	35
9. ¹ H and ¹³ C NMR spectra for organic compounds.....	36
9. References	44

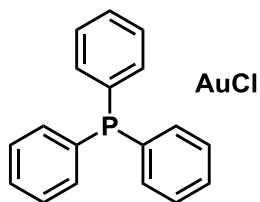
1. General experimental procedures

Unless stated otherwise, all reagents were purchased from commercial sources (Sigma Aldrich UK, Alfa Aesar UK, Acros UK or Apollo Scientific) and used without further purification. Commercial citrate-stabilized nanoparticle (NP) samples were purchased from BBI Scientific and used as supplied. Dry solvents were obtained by means of a MBBRAUN MB SPS-800™ solvent purification system, where solvents were passed through filter columns and dispensed under an argon atmosphere. Nanopure water from an Elga PURELAB Classic system was used throughout for all NP work. Flash column chromatography was performed using Geduran® Si60 (40-63 μm , Merck, Germany) as the stationary phase, and thin-layer chromatography (TLC) was performed on pre-coated silica gel plates (0.25 mm thick, 60F₂₅₄, Merck, Germany) and observed under UV light (λ_{max} 254 nm), or visualized by staining with a basic potassium permanganate solution, followed by heating. AuNP micrographs were obtained using a JEM 2010 TEM on samples prepared by deposition of one drop of nanoparticle suspension on Holey Carbon Films on 300 mesh Cu grids (Agar Scientific®). NP diameters were measured automatically using the software *ImageJ*. The images were first converted to black and white images using the “Threshold” function. The area of the NPs was measured using the “Analyze particles” function. Particles on edges were excluded. UV-vis spectroscopy was performed using a Thermo Scientific Evolution Array UV-Visible Spectrophotometer. ¹H, ¹³C, and ³¹P NMR spectra were recorded on Bruker Avance II 300, 400 and 500 instruments, at a constant temperature of 25 °C. ¹H chemical shifts are reported in parts per million (ppm) from low to high field and referenced to the literature values for chemical shifts of residual non-deuterated solvent, with respect to tetramethylsilane. ³¹P NMR chemical shifts are referenced to PPh₃ (–6.00 ppm) as external standard. Standard abbreviations indicating multiplicity are used as follows: bs (broad singlet), d (doublet), dd (doublet of doublets), m (multiplet), q (quartet), s (singlet), t (triplet), tt (triplet of triplets), *J* (coupling constant). All spectra were analyzed using MestReNova (Version 9.0.0). All melting points were determined using a Stuart SMP30 Melting Point Apparatus and are reported uncorrected. DLS measurements were performed on a Malvern Zetasizer μV instrument, with three replicates of 10–15 runs used throughout. The number of runs was determined automatically.

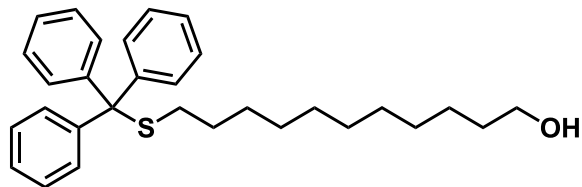
2. Synthesis of organic compounds



Scheme S1 Reagents and conditions for synthesis of disulfide/thiol ligands **1₂**, **1H** and **2H**. (i) NaOH/H₂O, Ph₃CSH, EtOH, PhMe, 5 h, RT, 99%. (ii) MsCl, Et₃N, CH₂Cl₂, 3 h, 0 °C, 99%. (iii) NaOH/H₂O, tetraethylene glycol, 100 °C, 24 h, 81%. (iv) MsCl, Et₃N, CH₂Cl₂, 18 h, 0 °C, 99%. (v) 1. NaH, THF, 96 h, reflux; 2. HCl/H₂O, MeOH, RT, 3 h, 15%. (vi) I₂, MeOH, 4 h, RT, 74%. (vii) CF₃CO₂H, ⁱPr₃SiH, CH₂Cl₂, 5 h, RT, 88%. (viii) CF₃CO₂H, ⁱPr₃SiH, CH₂Cl₂, 5 h, RT, 84%.

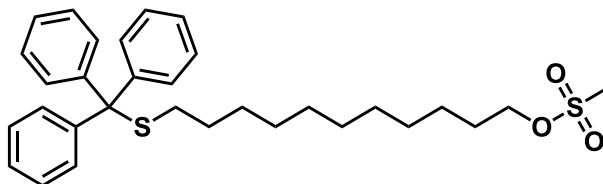
Compound S1: Chloro(triphenylphosphine)gold(I)

A solution of PPh₃ (735 mg, 2.80 mmol) in diethyl ether (10 mL) was added dropwise to a solution of HAuCl₄·3H₂O (500 mg, 1.47 mmol) in diethyl ether (30 mL). The reaction mixture was stirred at 0 °C for three hours, and then allowed to warm to RT. The resulting white precipitate was filtered and washed with cold Et₂O to give an off-white solid. This solid was recrystallized from CH₂Cl₂/hexane to give the desired gold complex **S1** as a crystalline white solid (500 mg, 1.01 mmol, 69%); M.p.: 236–237 °C; ¹H NMR (300.1 MHz, CDCl₃): δ 7.55–7.45 (15H, m, ArH); ¹³C NMR (125.8 MHz, CDCl₃): δ 134.4–134.1 (d, *J* = 13.7 Hz), 132.3–132.0 (d, *J* = 2.5 Hz), 129.5–129.3 (d, *J* = 11.8 Hz), 129.1–128.4 (d, *J* = 96.7 Hz); ³¹P NMR (121.5 MHz, CDCl₃): δ 33.5 (1P, s); HRMS (ES⁺) *m/z* calculated for [M+Na]⁺ C₁₈H₁₅AuClNaP 517.0158, found 517.0162.

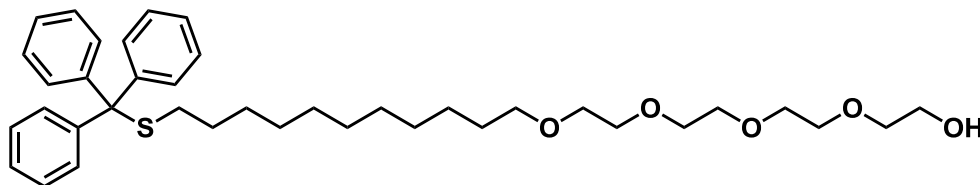
Compound S2: 11-(tritylthio)undecan-1-ol

A solution of NaOH (2.67 g, 66.8 mmol) in H₂O (25 mL) was added to a solution of triphenylmethanethiol (12.3 g, 44.5 mmol) in a mixture of EtOH/PhMe (1:1 v/v, 100 mL). 11-Bromo-1-undecanol (11.2 mg, 44.5 mmol) was dissolved in a second solution of EtOH/PhMe (1:1 v/v, 100 mL), which was then added to the triphenylmethanethiol mixture in one portion. The reaction mixture was stirred for 18 hours at RT. The mixture was poured into a saturated solution of NaHCO₃ (50 mL) and extracted with Et₂O (3 × 40 mL). The combined organic layers were washed with brine (3 × 40 mL), dried over MgSO₄ and solvent was removed under vacuum to give a pale yellow oil. The crude product was purified by flash column chromatography (SiO₂, hexane/EtOAc, 8:1 → 1:1) to give the desired product **S2** as a pale yellow oil (17.4 g, 39.0 mmol, 88%, spectral data in agreement with the literature^[S1]); ¹H NMR (500.1 MHz, CDCl₃): δ 7.46–7.43 (6H, dd, *J* = 9.0 Hz, *J* = 1.5 Hz, ArH), 7.19–7.34 (9H, m, ArH), 3.66 (2H, t, *J* = 7.5 Hz, CH₂OH), 2.16 (2H, t, *J* = 7.5 Hz, CH₂S), 1.59 (2H, qn, *J* = 7.5 Hz, CH₂), 1.44–1.20 (16H, m, CH₂); ¹³C NMR (125.8 MHz, CDCl₃): δ 145.2 (ArC_q), 129.7 (ArCH), 127.9 (ArCH), 126.6 (ArCH), 66.4 (C_q), 63.1 (CH₂O), 34.2 (CH₂S), 32.9 (CH₂), 32.1 (CH₂), 29.7 (CH₂), 29.6 (CH₂), 29.5 (CH₂), 29.3 (CH₂), 29.1 (CH₂), 28.7 (CH₂), 25.8 (CH₂).

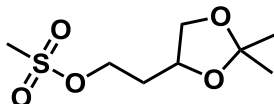
Compound S3: 11-(tritylthio)undecyl methanesulfonate



A solution of 11-(tritylthio)undecan-1-ol **S2** (17.4 g, 39.0 mmol) and triethylamine (6.70 g, 58.5 mmol) in dry CH_2Cl_2 (100 mL) was cooled to 4 °C and stirred under argon. Methanesulfonyl chloride (7.89 g, 78.0 mmol) in dry CH_2Cl_2 (50 mL) was added dropwise, while maintaining the temperature below 5 °C. The reaction mixture was stirred for 30 minutes at 4 °C and then allowed to warm to RT and stirred for a further 2 hours. Solvent was then removed under reduced pressure. The resulting residue was redissolved in CH_2Cl_2 (30 mL) and washed with 0.1 M HCl (2 × 20 mL), saturated NaHCO_3 solution (3 × 20 mL), and brine (2 × 20 mL). The organic layer was dried over Na_2SO_4 and concentrated under reduced pressure to give the desired product **S3** as a yellow oil (19.4 g, 36.9 mmol, 95%, spectral data in agreement with the literature^[S1]); ^1H NMR (500.1 MHz, CDCl_3): δ 7.44 (6H, dd, $J = 6.0$ Hz, $J = 1.5$ Hz, ArH), 7.33–7.20 (9H, m, ArH), 4.24 (2H, t, $J = 6.0$ Hz, CH_2O), 3.02 (3H, s, CH_3), 2.16 (2H, t, $J = 7.5$ Hz, CH_2S), 1.77 (2H, qn, $J = 6.0$ Hz, CH_2), 1.44–1.20 (16H, m, CH_2); ^{13}C NMR (125.8 MHz, CDCl_3): δ 145.2 (ArC_q), 129.7 (ArCH), 127.9 (ArCH), 126.6 (ArCH), 70.3 (CH_2O), 66.5 (C_q), 52.7 (CH_3), 37.5 (CH_2S), 32.1 (CH_2), 29.5 (CH_2), 29.5 (CH_2), 29.3 (CH_2), 29.2 (CH_2), 29.1 (CH_2), 29.1 (CH_2), 28.7 (CH_2), 25.5 (CH_2).

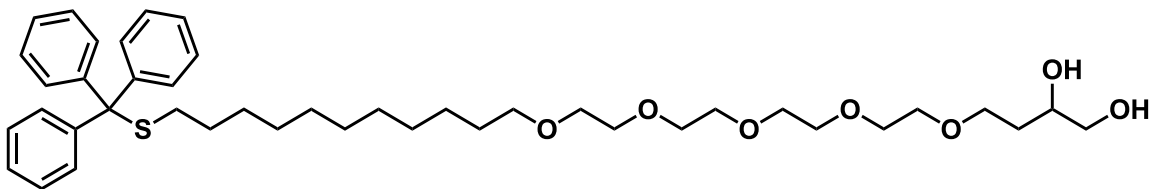
Compound S4: 1,1,1-triphenyl-14,17,20,23-tetraoxa-2-thiapentacosan-25-ol

NaOH (1.90 g, 47.4 mmol) in H₂O (2 mL) was added to tetraethylene glycol (140 g, 720 mmol) and stirred for 1 hour at 90 °C. 11-(tritylthio)undecyl methanesulfonate **S3** (22.6 g, 43.1 mmol) was added to the reaction mixture and stirred for 24 h at 90 °C (monitored by TLC, hexane/EtOAc, 1:2). After cooling to RT, the reaction mixture was poured into H₂O (200 mL) and extracted with Et₂O (5 × 100 mL), washed with saturated NaHCO₃ (3 × 50 mL) and brine (3 × 50 mL), dried over MgSO₄ and evaporated under vacuum to give the desired product **S4** as a yellow oil (20.3 g, 32.5 mmol, 76%, spectral data in agreement with the literature^[S1]); ¹H NMR (300.1 MHz, CDCl₃): δ 7.42 (6H, dd, *J* = 6.9 Hz, *J* = 1.5 Hz, ArH), 7.32–7.18 (9H, m, ArH), 3.74 (2H, t, *J* = 4.4 Hz, CH₂OH), 3.69–3.57 (14H, m, OCH₂CH₂O), 3.45 (2H, t, *J* = 6.9 Hz, CH₂O), 2.13 (2H, t, *J* = 7.5 Hz, CH₂S), 1.62–1.53 (2H, m, CH₂), 1.43–1.11 (16H, m, CH₂); ¹³C NMR (75.5 MHz, CDCl₃): δ 145.2 (ArC_q), 129.7 (ArCH), 127.9 (ArCH), 126.6 (ArCH), 72.7 (CH₂O), 71.7 (CH₂O), 70.8 (CH₂O), 70.8 (CH₂O), 70.7 (CH₂O), 70.7 (CH₂O), 70.5 (CH₂O), 70.2 (CH₂O), 66.5 (C_q), 61.9 (CH₂O), 32.2 (CH₂S), 29.7 (CH₂), 29.7 (CH₂), 29.6 (CH₂), 29.6 (CH₂), 29.5 (CH₂), 29.3 (CH₂), 29.2 (CH₂), 28.7 (CH₂), 26.2 (CH₂); MS (ES⁺) *m/z* 644.93 ([M+Na]⁺, 100).

Compound S5: 2-(2,2-dimethyl-1,3-dioxolan-4-yl)ethyl methanesulfonate

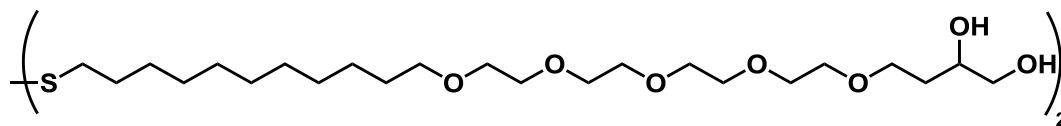
To a solution of 4-(2-hydroxyethyl)-2,2-dimethyl-1,3-dioxolane (5.00 g, 30.5 mmol) and Et₃N (3.69 g, 36.5 mmol) in CH₂Cl₂ (60 mL) at 0 °C was added dropwise a solution of methanesulfonyl chloride (4.18 g, 36.5 mmol) in CH₂Cl₂ (20 mL). The reaction mixture was stirred at 0 °C for 1.5 h, then H₂O (20 mL) was added. The organic layer was separated, washed with saturated Na₂CO₃ (2 × 30 mL) and brine (2 × 30 mL), dried over MgSO₄ and concentrated under reduced pressure to give compound **S5** as a yellow oil (5.86 g, 26.1 mmol, 91%, spectral data in agreement with the literature^[S2]); ¹H NMR (300.1 MHz, CDCl₃): δ 4.43–4.30 (2H, m, CH₂O), 4.27–4.18 (1H, m, CH), 4.10 (1H, dd, *J* = 8.1 Hz and *J* = 6.0 Hz, CH₂), 3.60 (1H, dd, *J* = 8.1 Hz, *J* = 6.5 Hz, CH₂'), 3.02 (3H, s, CH₃), 2.08 – 1.89 (2H, m, CH₂), 1.41 (3H, s, CH₃), 1.35 (3H, s, CH₃); ¹³C NMR (CDCl₃, 75.5 MHz): δ 109.7 (C_q), 72.3 (CH), 69.3 (CH₂), 67.2 (CH₂), 37.5 (SCH₃), 33.6 (CH₂), 27.1 (CH₃), 25.7 (CH₃).

Compound S6: 1,1,1-triphenyl-14,17,20,23,26-pentaoxa-2-thiatriacontane-29,30-diol

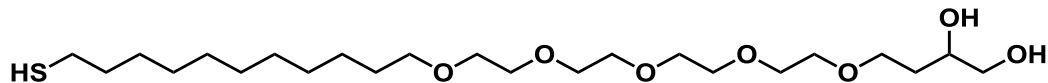


NaH (0.732 g, 60% dispersion in mineral oil, 18.3 mmol) was added to a solution of trityl protected hydroxythiol **S4** (7.60 g, 12.2 mmol) in dry THF (100 mL) and stirred for 1 hour at 50 °C under argon. To this reaction mixture, methanesulfonate **S5** (3.00 g, 13.4 mmol) was added and refluxed for 18 h (monitored by TLC, hexane/EtOAc, 1:2). The reaction mixture was quenched with saturated ammonium chloride, and the volume of solvent was reduced to about 10 mL under vacuum. The residue was diluted with EtOAc (50 mL) and washed with sat. NaHCO₃ (3 × 20 mL) and brine (2 × 30 mL), dried over MgSO₄ and solvent removed under vacuum. The residue was partially purified by column chromatography (hexane/EtOAc, 1:2) to give the intermediate acetal as a pale yellow oil. ¹H NMR (500.1 MHz, CDCl₃): δ 7.42–7.40, (6H, m, ArH), 7.29–7.26, (6H, m, ArH), 7.21–7.18, (3H, m, ArH), 4.21–4.16 (1H, m, CH), 4.07–4.05 (1H, m, CH₂), 3.82–3.77 (1H, m, CH₂'), 3.65–3.50, (18H, m, CH₂O), 3.44 (2H, t, *J* = 7.5 Hz, CH₂O) 2.12 (2H, t, *J* = 7.5 Hz, CH₂S), 1.59–1.53 (4H, m, CH₂), 1.43–1.08 (2H, m, CH₂), 1.43 (16H, m, CH₂), 1.40 (3H, s, CH₃), 1.35 (3H, s, CH₃).

The oil was dissolved in MeOH (100 mL) and conc. HCl (10 mL) was added. The mixture was stirred at RT for one hour and then neutralized with NaHCO₃. The volume of solvent was reduced to approximately 20 mL under vacuum, and subsequently the remaining cloudy solution was diluted with water (20 mL) and extracted with CH₂Cl₂ (3 × 50 mL). The combined organic layers were washed with brine (3 × 30 mL) and dried over MgSO₄. Solvent was removed under vacuum to give **S6** as a pale yellow oil. (1.95 g, 2.75 mmol, 15%); ¹H NMR (300.1 MHz, CDCl₃): δ 7.43–7.39, (6H, m, ArH), 7.32–7.26, (6H, m, ArH), 7.26–7.18, (3H, m, ArH), 3.96–3.88 (1H, m, CH), 3.76–3.57, (18H, m, CH₂O), 3.47–3.42 (4H, m, CH₂O) 2.13 (2H, t, *J* = 7.5 Hz, CH₂S), 1.78–1.70 (2H, m, CH₂), 1.62–1.53 (2H, m, CH₂), 1.43 (16H, m, CH₂); ¹³C NMR (CDCl₃, 75.5 MHz): δ 145.2 (ArC), 129.7 (ArCH), 127.9 (ArCH), 126.6 (ArCH), 71.7 (CH₂O), 70.9 (CHO), 70.9 (CH₂O), 70.7 (CH₂O), 70.7 (CH₂O), 70.7 (CH₂O), 70.7 (CH₂O), 70.7 (CH₂O), 70.5 (CH₂O), 70.3 (CH₂O), 70.1 (CH₂O), 68.9 (CH₂O), 66.7 (C_q), 32.9 (CH₂S), 32.2 (CH₂), 29.7 (CH₂), 29.7 (CH₂), 29.6 (CH₂), 29.6 (CH₂), 29.5 (CH₂), 29.3 (CH₂), 29.2 (CH₂), 28.7 (CH₂), 26.2 (CH₂); MS (ES⁺) *m/z* 733.24 ([M+Na]⁺, 100), (ES⁻) *m/z* 745.29 ([M+³⁵Cl]⁻, 100), 747.34 ([M+³⁷Cl]⁻, 30); HRMS (ES⁺) *m/z* calculated for [M+Na]⁺ C₄₂H₆₂NaO₇S⁺ 733.4108, found 733.4116.

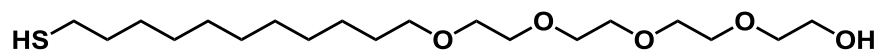
Compound 1₂: 5,8,11,14,17,42,45,48,51,54-decaoxa-29,30-dithiaoctapentacontane-1,2,57,58-tetraol

Trityl protected thiol **S6** (200 mg, 0.281 mmol) was dissolved in MeOH (8 mL) and I₂ (143 mg, 0.563 mmol) was added. The reaction was stirred at RT for 4 hours. The solution was then decolorized by addition of an aqueous sat. sodium sulfite solution until no brown color persisted. Solvent was removed under reduced pressure, and the residue was redissolved in CH₂Cl₂ (20 mL), washed with sat. NaHCO₃ (3 × 25 mL) and brine (3 × 25 mL). The resulting oil was dissolved in hexane/EtOAc (1:2) and loaded onto a short plug of silica, washing with more of the same solvent. The desired pure product was eluted using methanol and dried under vacuum to give **1₂** as a pale yellow oil. (108 mg, 0.230 mmol, 82%); ¹H NMR (500.1 MHz, CDCl₃): δ 3.95–3.87 (2H, m, CHOH), 3.71–3.55 (36H, m, CH₂O), 3.51–3.41 (8H, m, CH₂O), 2.76 (8H, bs, OH), 2.67 (4H, t, *J* = 7.5 Hz, CH₂O), 1.76–1.52, (4H, m, CH₂), 1.38–1.19, (28H, m, CH₂); ¹³C NMR (CDCl₃, 125.8 MHz): δ 71.7 (CH₂O), 70.9 (CHO), 70.9 (CH₂O), 70.7 (CH₂O), 70.7 (CH₂O), 70.7 (CH₂O), 70.7 (CH₂O), 70.5 (CH₂O), 70.3 (CH₂O), 70.1 (CH₂O), 68.9 (CH₂O), 66.7 (CH₂O), 39.3 (CH₂S), 32.9 (CH₂), 29.7 (CH₂), 29.7 (CH₂), 29.7 (CH₂), 29.6 (CH₂), 29.6 (CH₂), 29.4 (CH₂), 29.3 (CH₂), 28.7 (CH₂), 26.2 (CH₂); MS (ES⁺) *m/z* 952.64 ([M+NH₄]⁺, 100), 957.60 ([M+Na]⁺, 100), (ES⁻) *m/z* 969.51 ([M+³⁵Cl]⁻, 100), 971.63 ([M+³⁷Cl]⁻, 30); HRMS (ES⁺) *m/z* calculated for [M+NH₄]⁺ C₄₆H₉₄O₁₄S₂NH₄⁺ 952.6423, found 952.6422, calculated for [M+Na]⁺ C₄₆H₉₄O₁₄S₂Na⁺ 957.5977, found 957.5971.

Compound 1H: 28-mercapto-5,8,11,14,17-pentaoxaoctacosane-1,2-diol

Trityl protected thiol **S6** (500 mg, 0.700 mmol) was dissolved in dry CH₂Cl₂ (10 mL) and an excess of trifluoroacetic acid (1.60 g, 14.1 mmol) was added. Subsequently triisopropylsilane (133 mg, 0.840 mmol) was added and the reaction was stirred at room temperature under argon for 5 hours. Solvent and most of the CF₃CO₂H and *i*Pr₃SiH was distilled off at atmospheric pressure. The crude product was purified by column chromatography (hexane/EtOAc, 3:1 → 0:1) to give the desired product **1H** as a colorless oil (290 mg, 0.619 mmol, 88%); ¹H NMR (400.1 MHz, CDCl₃): δ 4.17–3.53 (21H, m), 3.40 (2H, t, *J* = 6.8 Hz, CH₂O), 2.51 (2H, dd, *J* = 7.2 Hz, *J* = 7.2 Hz, CH₂SH), 1.64–1.49 (4H, m, 2 × CH₂), 1.41 – 1.21 (14H, m, 7 × CH₂), 1.32 (1H, t, *J* = 8.0 Hz, SH); ¹³C NMR (75.5 MHz, CDCl₃): δ 71.5 (CH₂O), 71.1 (CH₂O), 70.8 (CH₂O), 70.8 (CH₂O), 70.6 (CH₂O), 70.4 (CH₂O), 69.9 (CH₂O), 69.1 (CH₂O), 69.0 (CH₂O), 69.0 (CH₂O), 69.6 (CHO), 63.0 (CH₂OH), 34.0 (CH₂SH), 29.5 (CH₂), 29.5 (CH₂), 29.5 (CH₂), 29.5 (CH₂), 29.5 (CH₂), 29.4 (CH₂), 29.0 (CH₂), 28.3 (CH₂), 26.0 (CH₂), 24.6 (CH₂); MS (ES⁺) *m/z* 491.42 ([M+Na]⁺, 100); HRMS (ES⁺) *m/z* calculated for [M+Na]⁺ C₂₃H₄₈O₇Na⁺ 491.3013, found 491.3002.

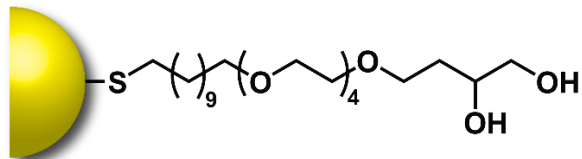
Compound 2H: 23-mercapto-3,6,9,12-tetraoxatricosan-1-ol



Trityl protected thiol **S4** (2.00 g, 3.21 mmol) was dissolved in dry CH_2Cl_2 (30 mL) and an excess of trifluoroacetic acid (7.32 g, 64.20 mmol) was added. Subsequently triisopropylsilane (0.61 g, 3.85 mmol) was added and the reaction was stirred at room temperature under argon for 5 hours. Solvent and most of the $\text{CF}_3\text{CO}_2\text{H}$ and $i\text{Pr}_3\text{SiH}$ was distilled off at atmospheric pressure. The crude product was purified by column chromatography (hexane/EtOAc, 3:1 \rightarrow 1:8) to give the desired product **2H** as a colorless oil (1.03 g, 2.71 mmol, 84%, spectral data in agreement with the literature^[S2]); ^1H NMR (300.1 MHz, CDCl_3): δ 4.51–4.48 (2H, m, CH_2O), 3.81–3.78 (2H, m, CH_2O), 3.68 – 3.56 (12H, M, $6 \times \text{CH}_2\text{O}$), 3.45 (2H, t, $J = 7.4$ Hz, CH_2OH), 2.51 (2H, tt, $J = 7.5$ Hz, $J = 7.5$ Hz, CH_2SH), 1.65–1.52 (4H, m, $2 \times \text{CH}_2$), 1.39 – 1.23 (14H, m, $7 \times \text{CH}_2$), 1.33 (1H, t, $J = 7.8$ Hz, SH); ^{13}C NMR (75.5 MHz, CDCl_3): δ 71.7 (CH_2O), 70.9 (CH_2O), 70.8 (CH_2O), 70.7 (CH_2O), 70.7 (CH_2O), 70.7 (CH_2O), 70.1 (CH_2O), 68.3 (CH_2O), 67.1 (CH_2OH), 34.2 (CH_2S), 29.7 (CH_2), 29.7 (CH_2), 29.6 (CH_2), 29.6 (CH_2), 29.2 (CH_2), 28.5 (CH_2), 26.2 (CH_2), 24.8 (CH_2); MS (ES^+) m/z 403.25 ($[\text{M}+\text{Na}]^+$, 100).

3. Nanoparticle synthesis and characterization

3.1 AuNP-1



Synthetic procedure

ClAuPPh₃ (**S1**) (200 mg, 0.404 mmol) and dihydroxy-disulfide **1**₂ (400 mg, 0.424 mmol) were dissolved in a mixture of MeCN/THF (1:1 v/v, 20 mL) and stirred at 55 °C. To this, borane *tert*-butylamine complex (350 mg, 4.04 mmol) was added as a powder. The mixture was stirred for 1 hour at 55 °C. After this time, the solution was allowed to cool to RT and a black-purple precipitate was observed. Solvent was decanted, and the precipitate was transferred to a vial washing with Et₂O. The solid was sonicated in Et₂O, allowed to settle and excess Et₂O was decanted. This ether wash process was repeated 10 times, after which the solid was dried in air to give the desired nanoparticles AuNP-1 as a black powder (112 mg); ¹H NMR (400.1 MHz, CDCl₃): δ 4.1–3.0 (bs, CH₂O), 2.0–0.5 (bs CH₂).

Characterization

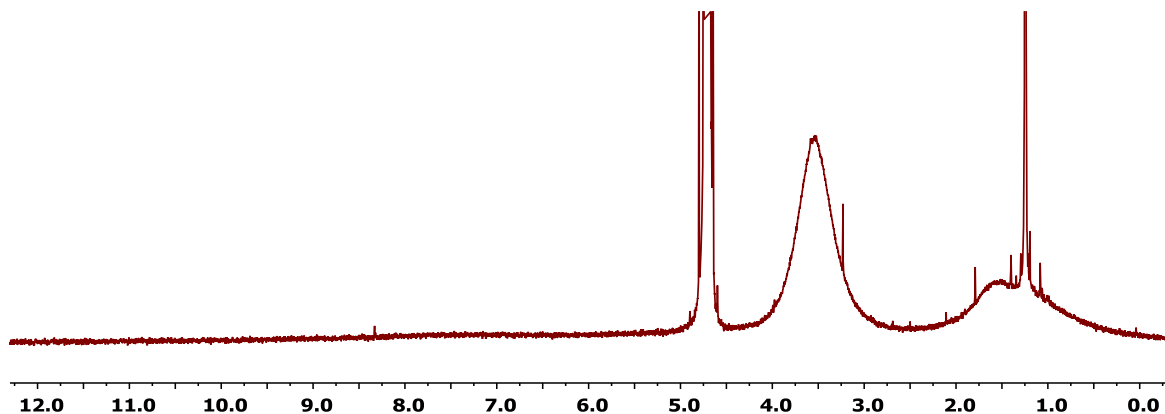


Figure S1 ¹H NMR spectrum (400.1 MHz, D₂O) of AuNP-1.

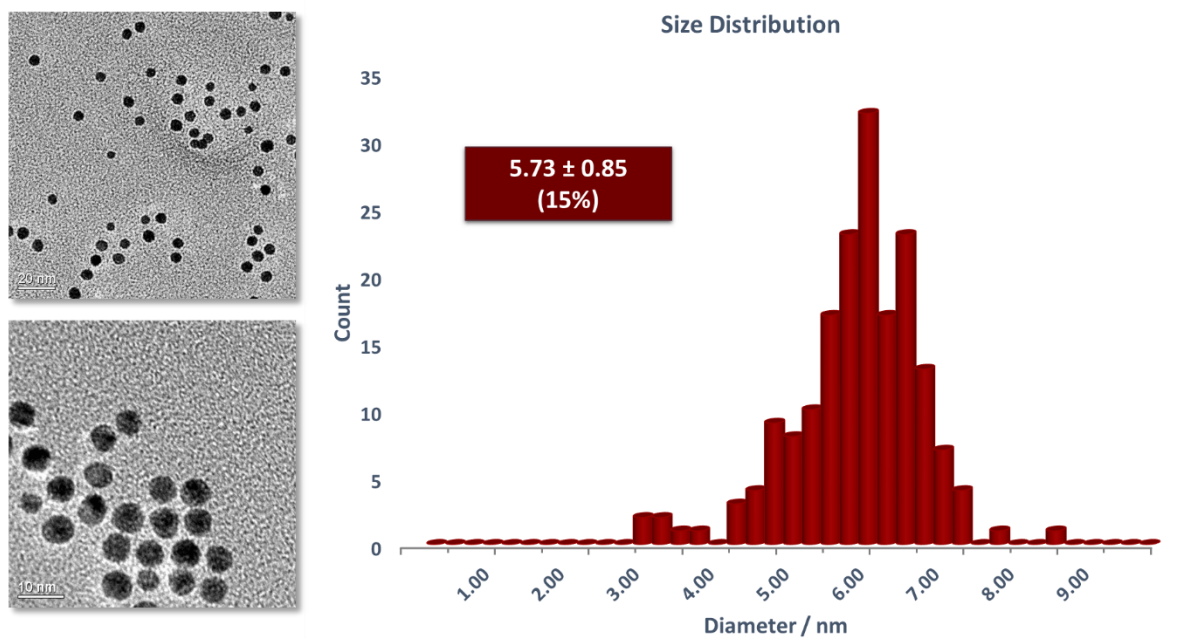


Figure S2 Representative TEM images of AuNP-1 and histogram of NP size distribution as found through analysis of several images using *ImageJ* software, as described in the general methods section. AuNP-1 were found to have a size of 5.73 ± 0.85 nm, corresponding to a dispersity of 15%.

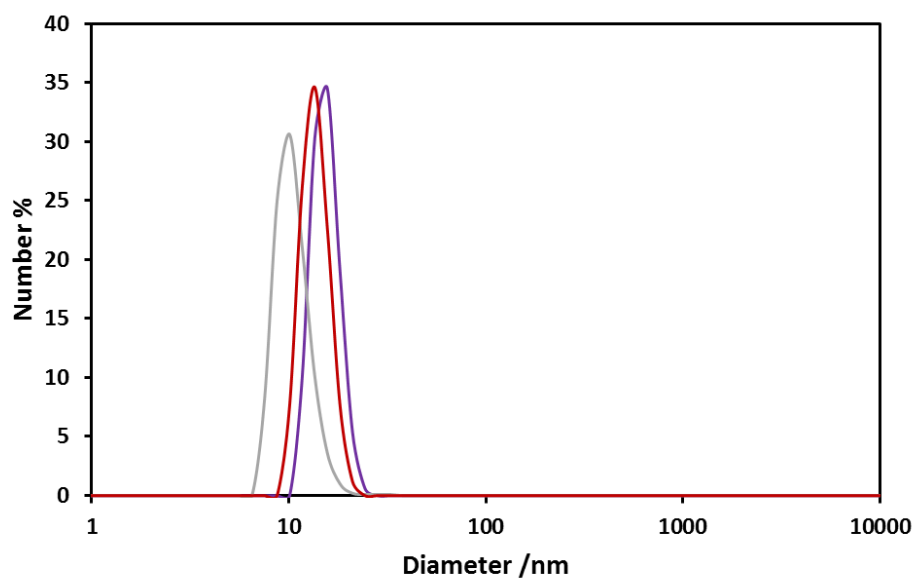


Figure S3 Dynamic light scattering measurements (H_2O , 25.0°C) of AuNP-1. Three replicate measurements gave an average hydrodynamic diameter of 13.7 nm.

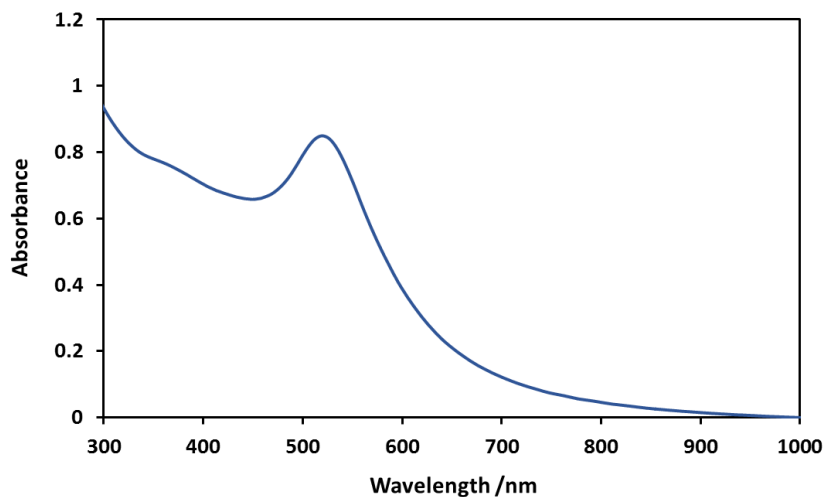
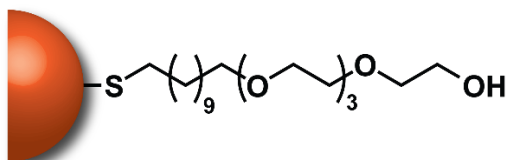


Figure S4 Extinction spectrum (H_2O , 20 °C) of AuNP-1, showing λ_{max} (SPR) = 519 nm.

3.2 AuNP-2



Synthetic procedure

ClAuPPh_3 **S1** (124 mg, 0.251 mmol) and hydroxy-thiol **2H** (200 mg, 0.526 mmol) were dissolved in THF (15 mL) and stirred at 55 °C. To this, borane *tert*-butylamine complex (218 mg, 2.507 mmol) was added as a powder. The mixture was stirred for 1 hour at 55 °C. After this time, the solution was allowed to cool to RT and a black-purple precipitate formed. Solvent was decanted, and the precipitate was transferred to a vial by washing with Et_2O . The solid was sonicated in Et_2O , allowed to settle, and excess ether decanted. This ether wash process was repeated 10 times, after which the solid was dried in air to give the desired nanoparticles AuNP-2 as a black powder (82 mg); ^1H NMR (400.1 MHz, CDCl_3): δ 4.0–3.3 (bs, CH_2O), 2.0–0.8 (bs CH_2).

Characterization

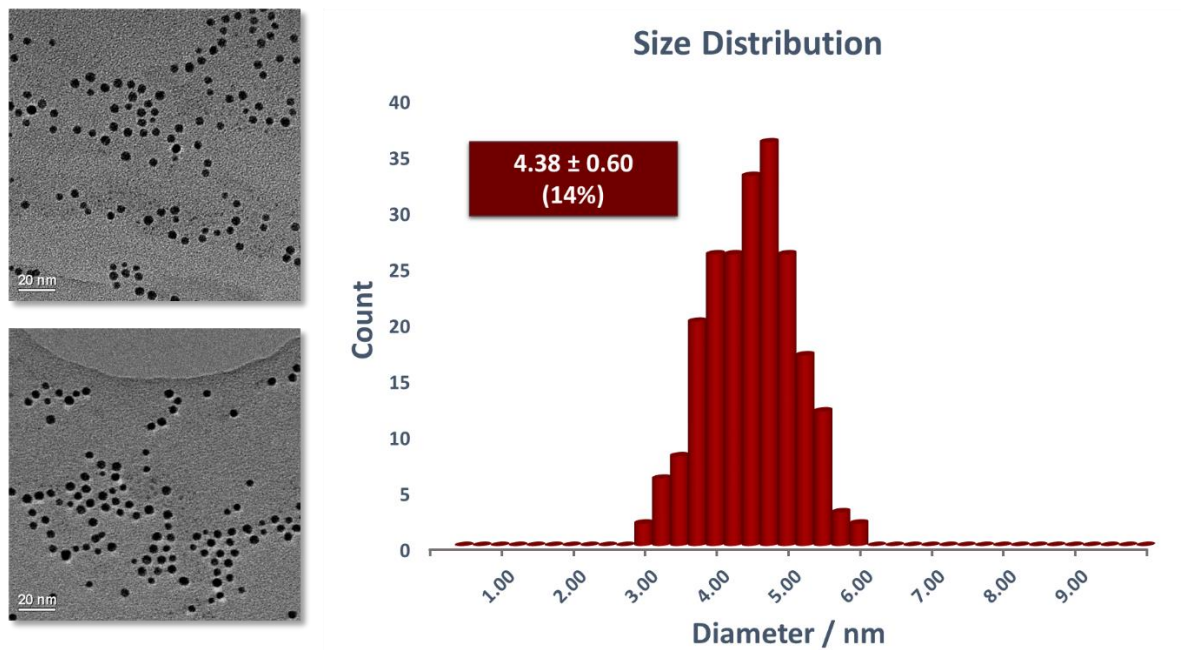


Figure S5 Representative TEM images of AuNP-2 and histogram of NP size distribution as found through analysis of TEM images using *ImageJ* software, as described in the general methods section. AuNP-2 were found to have a size of 4.38 ± 0.60 nm, corresponding to a dispersity of 14%.

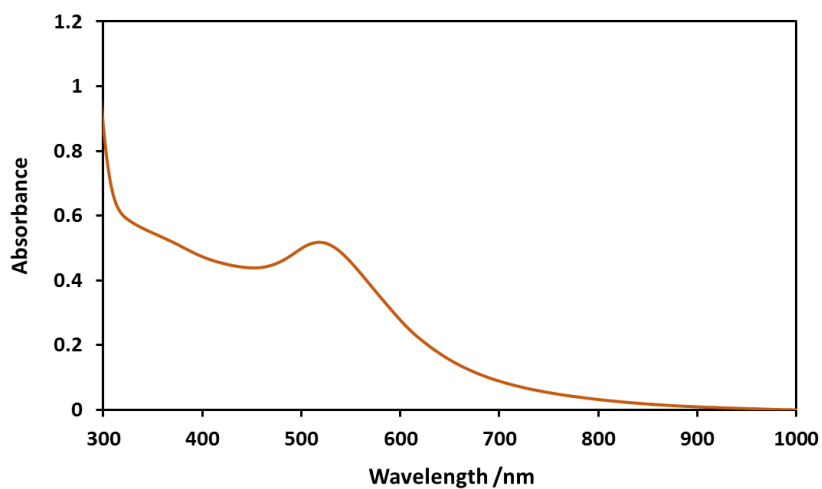
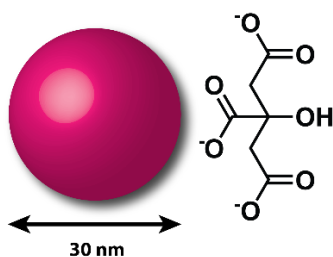


Figure S6 Extinction spectrum (H_2O , 20°C) of AuNP-2, showing λ_{max} (SPR) = 517 nm.

3.4 30 nm Citrate-stabilized NPs



Synthetic procedure^[S3]

Prior to synthesis, all glassware was cleaned rigorously with aqua regia, or, alternatively, new vials were used.

Three stock solutions were made up: **solution A**, $\text{HAuCl}_4 \cdot 3\text{H}_2\text{O}$ (25.0 mg, 0.0635 mmol) in H_2O (5 mL), **solution B**, silver nitrate (5.00 mg, 0.0294 mmol) in H_2O (5 mL), and **solution C**, trisodium citrate dihydrate (50.0 mg, 0.170 mmol) in H_2O (5 mL). Gold **solution A** (1000 μL) and silver **solution B** (43 μL) were added to citrate **solution C** (200 μL). Water (1260 μL) was subsequently added to give a total volume of 2.5 mL). The final quantities of each reagent were $\text{HAuCl}_4 \cdot 3\text{H}_2\text{O}$ (5.00 mg, 12.7 μmol), silver nitrate (0.0425 mg, 0.250 μmol) and trisodium citrate dihydrate (2.00 mg, 6.80 μmol). The combined solution was added to vigorously stirring boiling water (47.5 mL). The solution was heated to reflux for 1 hour, after which it was allowed to cool to RT and stored directly with no further work up.

Characterization

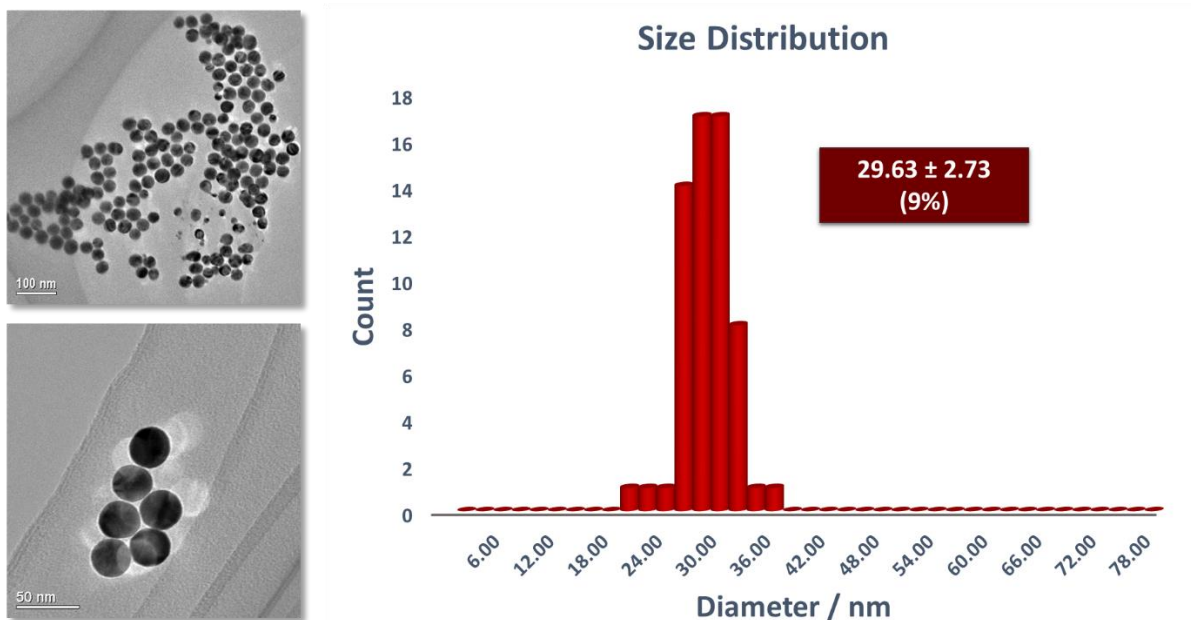


Figure S7 Representative TEM images of 30 nm citrate stabilized NP and histogram of NP size distribution as found through analysis of TEM images using *ImageJ* software, as described in the general methods section. NPs were found to have a size of 29.63 ± 2.73 nm, corresponding to a dispersity of 10%.

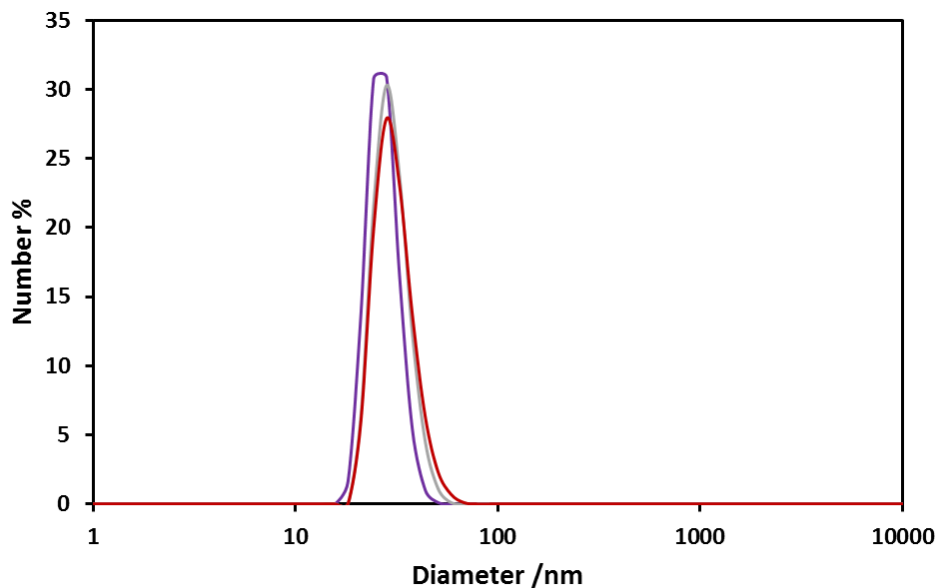


Figure S8 Dynamic light scattering measurements (H_2O , $25.0\text{ }^\circ\text{C}$) of 30 nm citrate-stabilized NPs. Three replicate measurements gave an average hydrodynamic diameter of 31.2 nm.

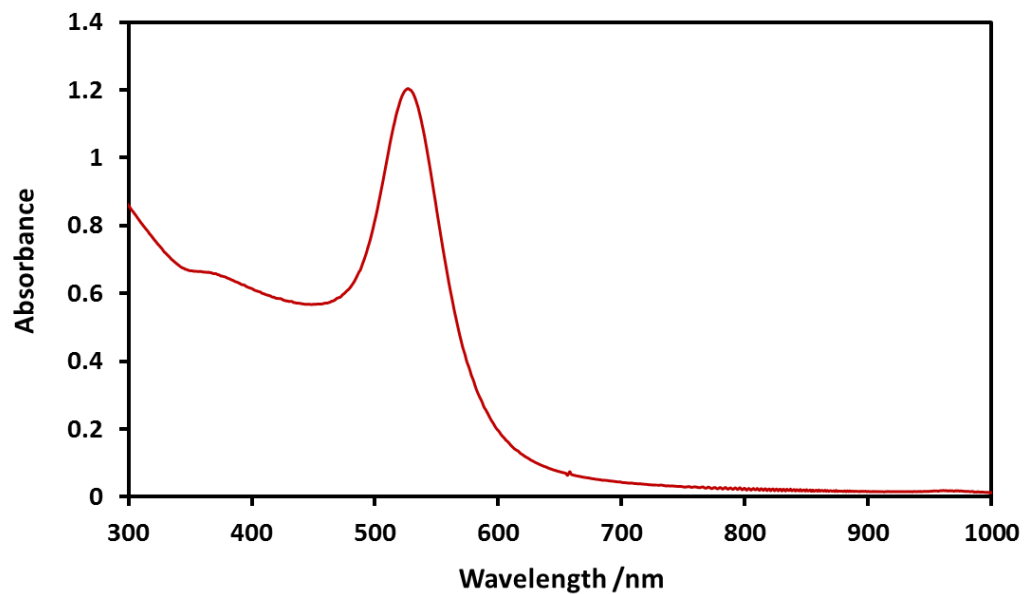


Figure S9 Extinction spectrum (H_2O , $20\text{ }^\circ\text{C}$) of 30 nm citrate-stabilized NPs, showing λ_{max} (SPR) = 529 nm.

3.5 Mixed shape citrate-stabilized NPs



Synthetic procedure

Prior to synthesis, all glassware was cleaned rigorously with aqua regia, or, alternatively, new vials were used.

$\text{HAuCl}_4 \cdot 3\text{H}_2\text{O}$ (21.6 mg, 0.050 mmol) was dissolved in H_2O (100 mL) and heated to reflux. Trisodium citrate dihydrate (113 mg, 0.384 mmol) was dissolved in H_2O (10 mL) and quickly added to the gold solution. The solution was heated for a further 10 minutes, when it initially turned black, and then gradually a deep red color. The reaction mixture was allowed to cool to RT. The solution contained 10 nm seed NPs, which were stored without further purification.

$\text{HAuCl}_4 \cdot 3\text{H}_2\text{O}$ (9.80 mg, 9.80 μmol) was dissolved in H_2O (100 mL). 10 nm seed NP solution (1 mL) was mixed with the $\text{HAuCl}_4 \cdot 3\text{H}_2\text{O}$ solution (9 mL) and stirred at room temperature for 7 hours, resulting in a disperse mixture of nanoparticles, containing significant populations of rods and prisms.

Characterization

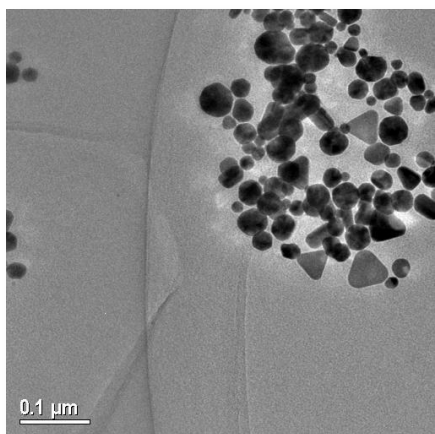


Figure S10 Representative TEM image of the solution of mixed shapes and sizes of citrate stabilized NPs, including spheres, rods and triangular prisms.

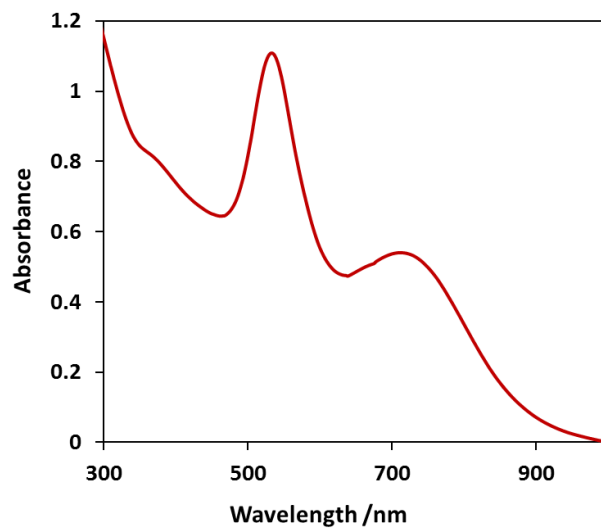


Figure S11 Extinction spectrum (H₂O, 20 °C) of mixed shapes and sizes of citrate stabilized NPs.

3.6 40 nm Commercial citrate stabilized NPs: Characterization

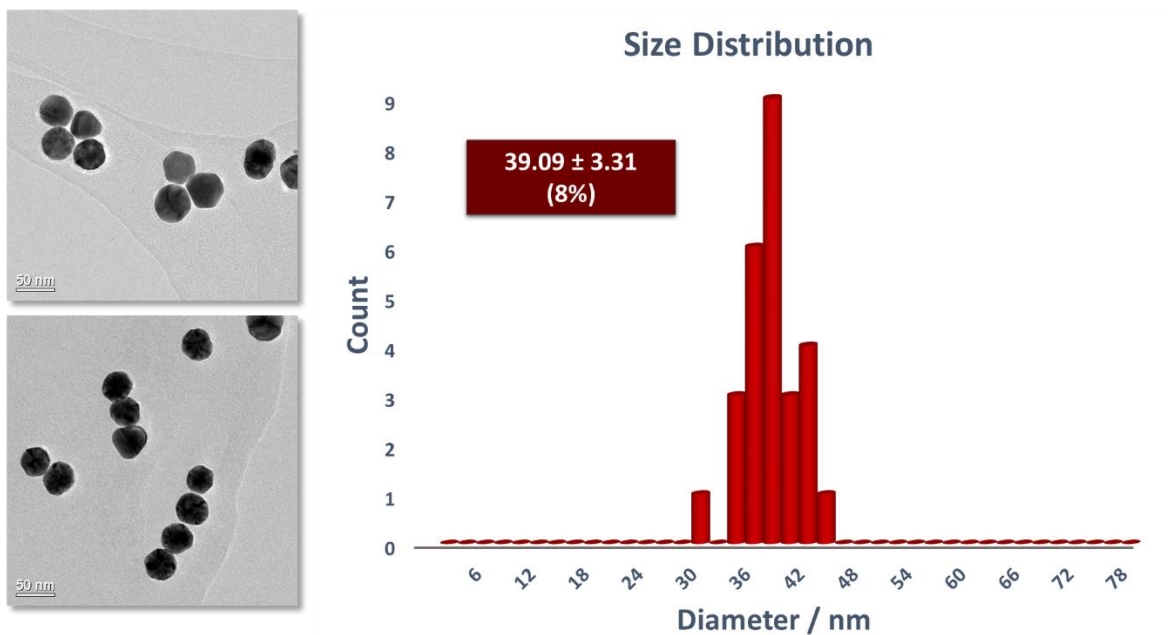


Figure S12 Representative TEM images of 40 nm commercial citrate-stabilized NPs and histogram of NP size distribution found through analysis of several such TEM images using *ImageJ* software, as described in the general methods section. The commercial citrate-stabilized NPs were found to have a size of 39.09 ± 3.31 nm, corresponding to a dispersity of 8%.

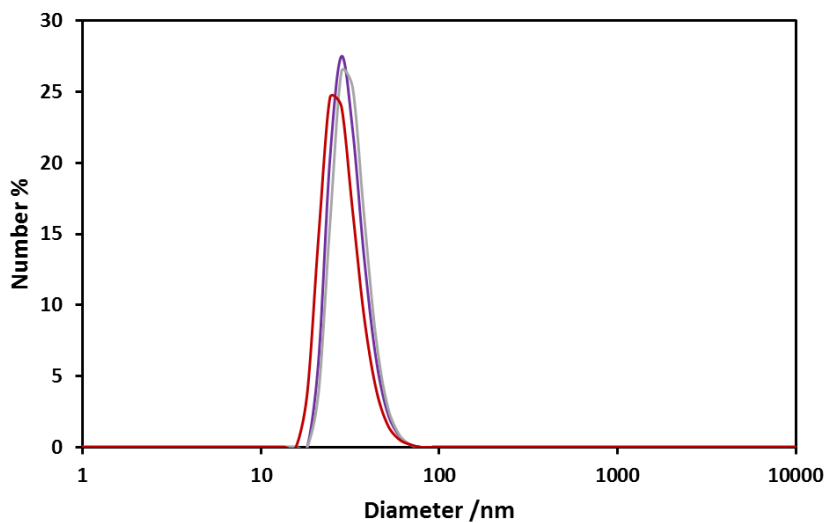


Figure S13 Dynamic light scattering measurements (H_2O , 25.0°C) of 40 nm commercial citrate-stabilized NPs. Three replicate measurements gave an average hydrodynamic diameter of 28.8 nm (Z-Average by Cumulants fit = 40.3 nm).

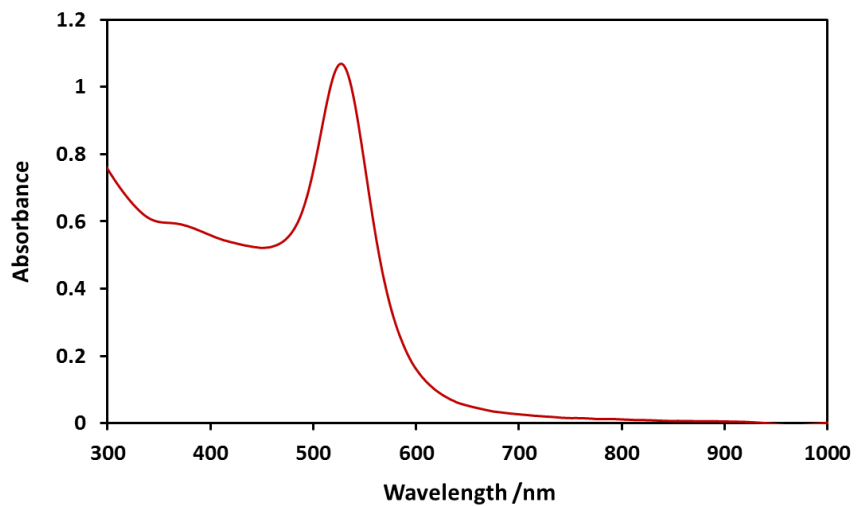


Figure S14 Extinction spectrum (H₂O, 20 °C) of 40 nm commercial citrate-stabilized NPs, showing λ_{max} (SPR) = 526 nm.

3.7 150 nm Commercial citrate stabilized NPs: Characterization

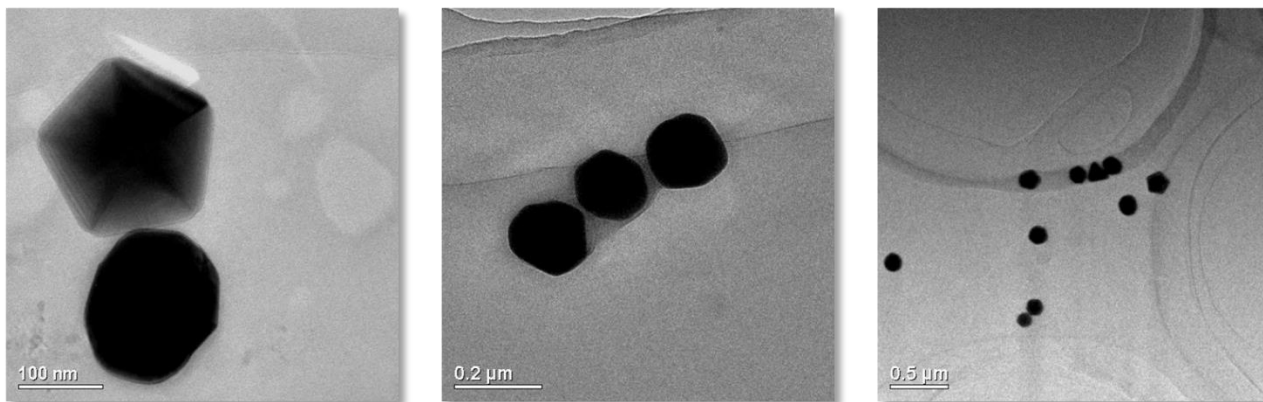


Figure S15 Representative TEM images of commercial 150 nm citrate-stabilized NPs.

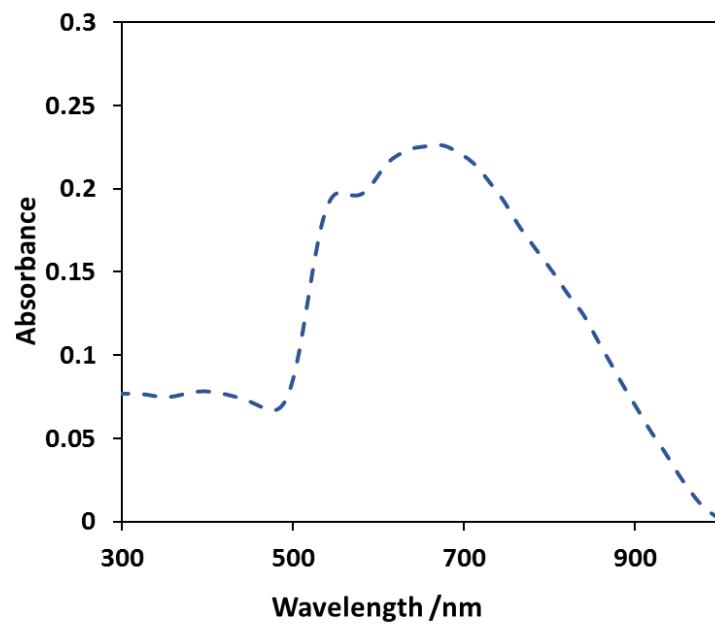


Figure S16 Extinction spectrum (H₂O, 20 °C) of 150 nm commercial citrate-stabilized NPs.

4. Determination of nanoparticle concentrations

Nanoparticle concentrations were derived from the UV-vis spectra, using **eq. s1**^[S4] to calculate the extinction coefficient (ϵ) at λ_{\max} (SPR), where d is the mean particle diameter in nm, $k = 3.32111$ and $a = 10.80505$.

$$\ln \epsilon = k \ln d + a \quad \text{eq. S1}$$

These extinction coefficients could then be used to calculate NP concentrations using the Beer-Lambert equation (**eq. s2**), where A is the measured absorbance at λ_{\max} (SPR), l is the path length of the cell (1 cm for all measurements) and c is the nanoparticle concentration.

$$A = \epsilon cl \quad \text{eq. S2}$$

Citrate stabilized NP solutions were used as made or as purchased. Thiol coated NPs were made up as 0.1 mg mL⁻¹ solutions in water and the concentrations subsequently determined from the UV-vis spectra. This gave the concentration values shown in the table below. For 150 nm citrate-stabilized NPs, the UV-Vis spectrum is dominated by scattering and so the concentration quoted by the manufacturer is used.

NPs	$\epsilon / \text{M}^{-1} \text{cm}^{-1}$	Concentration /nM
AuNP-1	1.624×10^7	54.4
40 nm commercial citrate stabilized NPs	9.550×10^{10}	0.112
30 nm citrate stabilized NPs	3.805×10^9	0.314
AuNP-2	6.652×10^6	77.8

For AuNP-1, an estimated concentration calculated from first principals is in reasonable agreement with the concentration determined from the plasmon absorbance.

Mean diameter (TEM)		5.73 nm
Radius		2.87 nm
Volume		98.5 nm ³
Surface Area		103 nm ²
NP core mass	(volume × density of Au (19.3 g cm ⁻³))	1.90 × 10 ⁻¹⁸ g
NP core molar mass	(NP core mass × N _A)	1.15 × 10 ⁶ g mol ⁻¹
Ligand molecular weight		468 g mol ⁻¹
	Assuming one ligand occupies ^[55] 0.214 nm ²	
Number of ligands per NP		482
NP ligand mass		2.25 × 10 ⁵ g mol ⁻¹
Total construct molar mass		1.37 × 10 ⁶ g mol ⁻¹
Concentration of nanoparticles in 0.1 mg mL ⁻¹ sample		73.0 nM

5. Planet–satellite preparation and purification

5.1 Synthetic procedure

In a standard procedure, an aqueous solution of dihydroxy-functionalized AuNP-1 (2.5 mL, 0.1 mg mL⁻¹, 54.4 nmol) were added to 40 nm citrate-stabilized NPs (6.5 mL, 0.112 nmol) in a vial. The vial was capped and shaken, and an immediate color change from red to purple was observed. The unpurified sample solution could be stored indefinitely.

To remove excess AuNP-1, the solution was centrifuged at 5900 rcf for 4 minutes. A dark solid was observed, and the remaining pale purple supernatant solution was decanted. Water was added to the original volume and the mixture was shaken and sonicated for 1 minute, resulting in complete redispersion of the solid. The sample was subsequently centrifuged again at 2900 rcf for 4 minutes, and the supernatant solution again decanted. Redispersion of the solid in the same volume of water gave a pure solution of the planet–satellite structures, which could be stored at room temperature in air indefinitely (≥ 12 months).

5.2 Determining the optimum mixing ratio

In order to establish the optimum stoichiometric ratio for planet–satellite assembly, the component NPs were mixed in different ratios, ranging from 14:1 to 2800:1 AuNP-1: citrate-NP. Monitoring the resulting assembly by UV-vis spectroscopy revealed a maximum red shift in the SPR maximum at around 280:1 (Figure S19). The initial increase in λ_{max} (SPR) with increasing satellite NPs is ascribed to increased coverage of the planet NPs leading to a larger average SPR shift for clusters in the sample. After reaching complete coverage around the 280:1 mixing ratio, the subsequent decrease in the λ_{max} (SPR) can be ascribed to the presence of increasing amounts of free AuNP-1 in solution, which begins to dominate the spectrum.

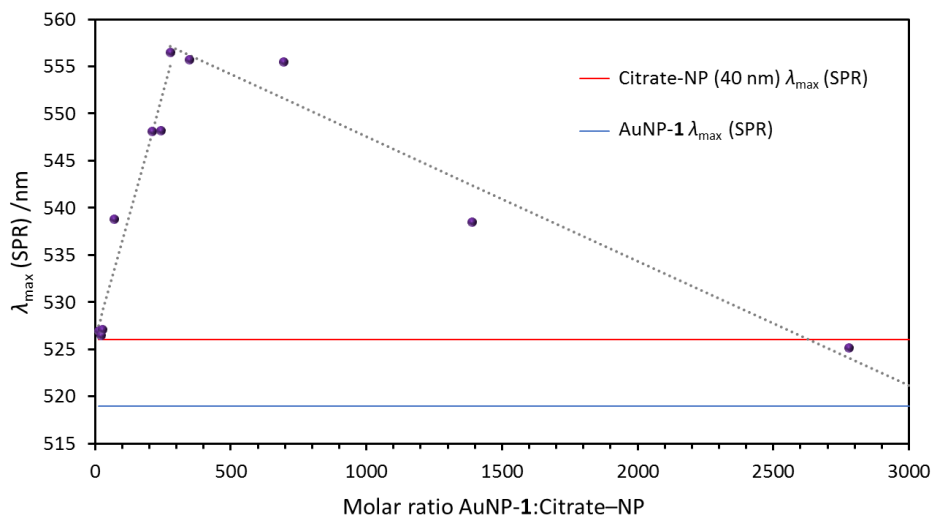


Figure S17 Plot of λ_{max} (SPR) observed for colloidal dispersions solutions with varying AuNP-1: citrate-NP (40 nm) ratio (H₂O, 20 °C). The maximum shift at a ratio of 280:1 reveals the optimum mixing ratio for planet–satellite formation. The solid red and blue lines indicate λ_{max} (SPR) of the component NPs in isolation; the dotted lines provide a guide for the eye.

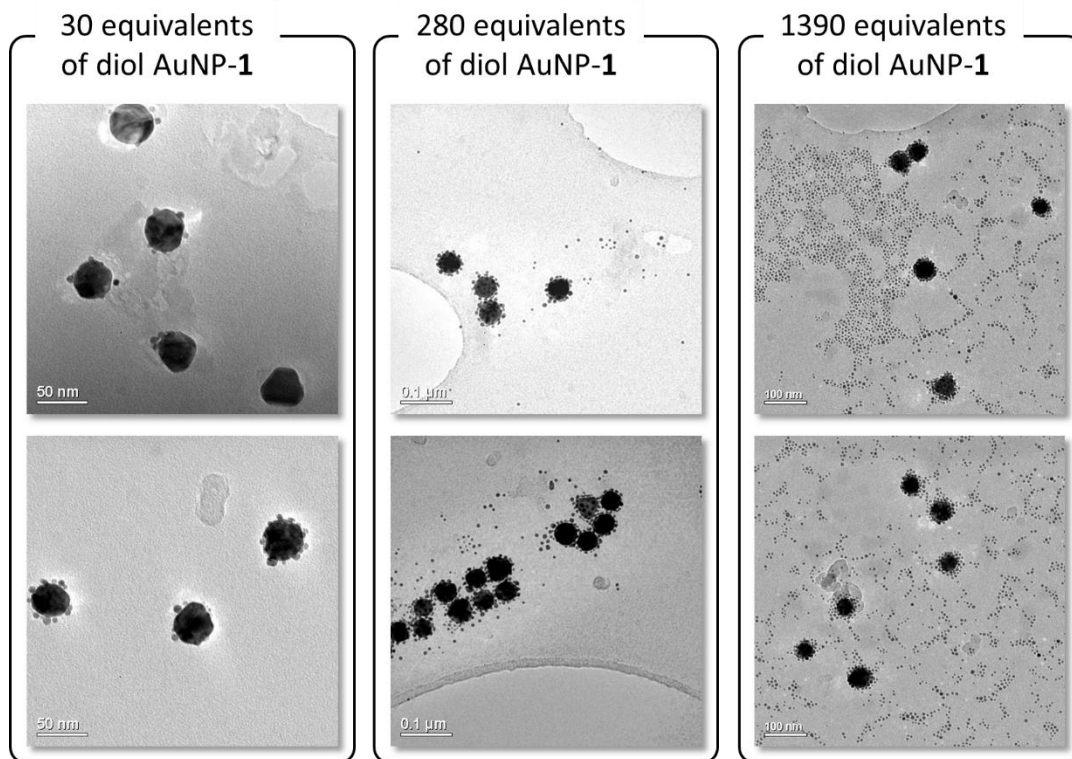


Figure S18 Representative TEM images of unpurified planet–satellite assembly samples at low (30:1), optimum (280:1) and high (1390:1) ratios of AuNP-1:citrate-NP. At 30 equivalents AuNP-1, incomplete satellite formation is observed; at 1390 equivalents, complete planet–satellite formation is observed, along with a large excess of AuNP-1; at 280 equivalents (the ratio corresponding to the maximum red shift in SPR maximum) complete satellite formation is observed and there is only a small excess of unbound AuNP-1.

5.3 Planet-satellite purification

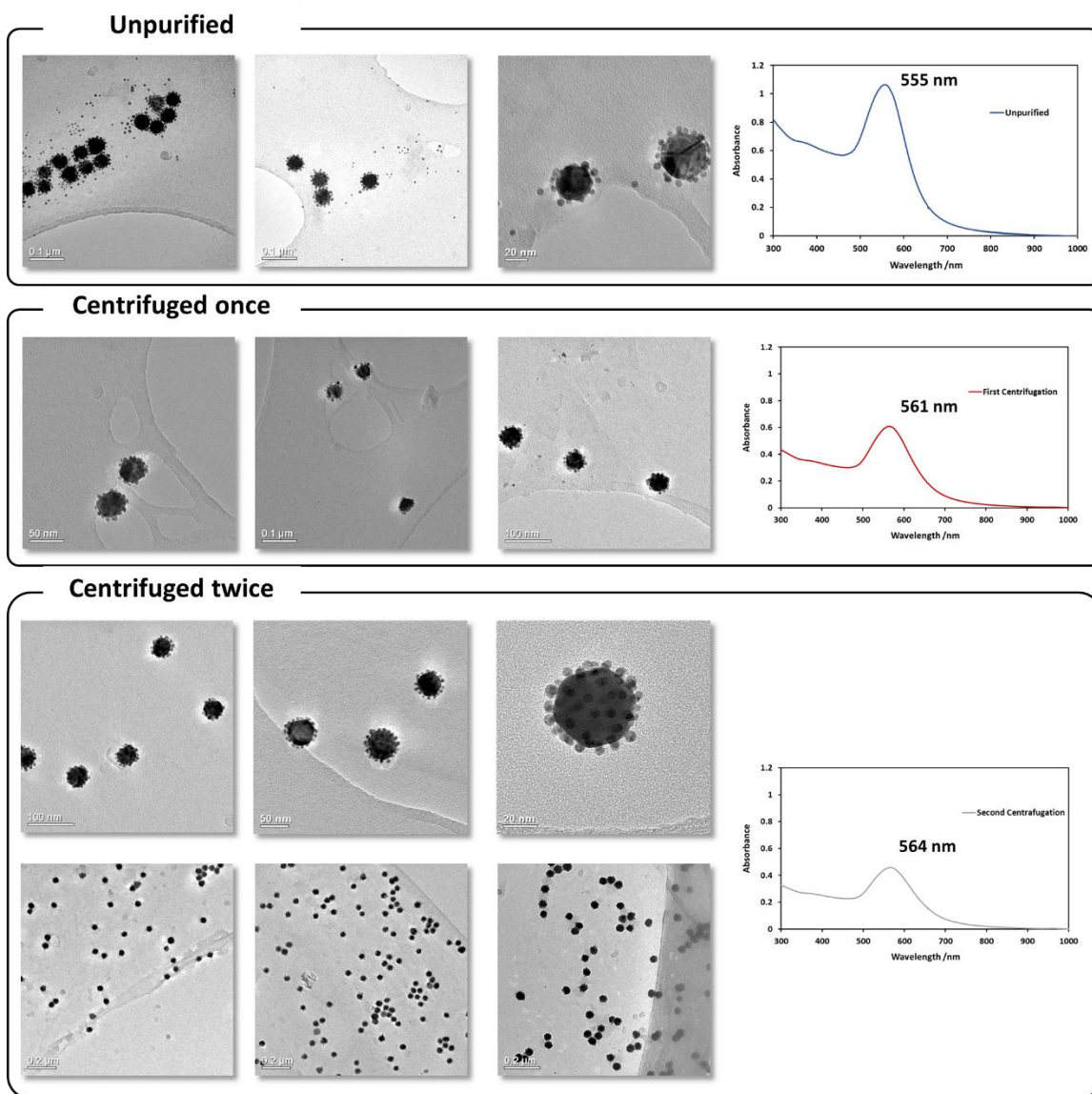


Figure S19 Representative TEM images and UV-vis spectra (H_2O , 20 $^\circ\text{C}$) of samples at each stage of the purification procedure, revealing the progressive removal of excess AuNP-1.

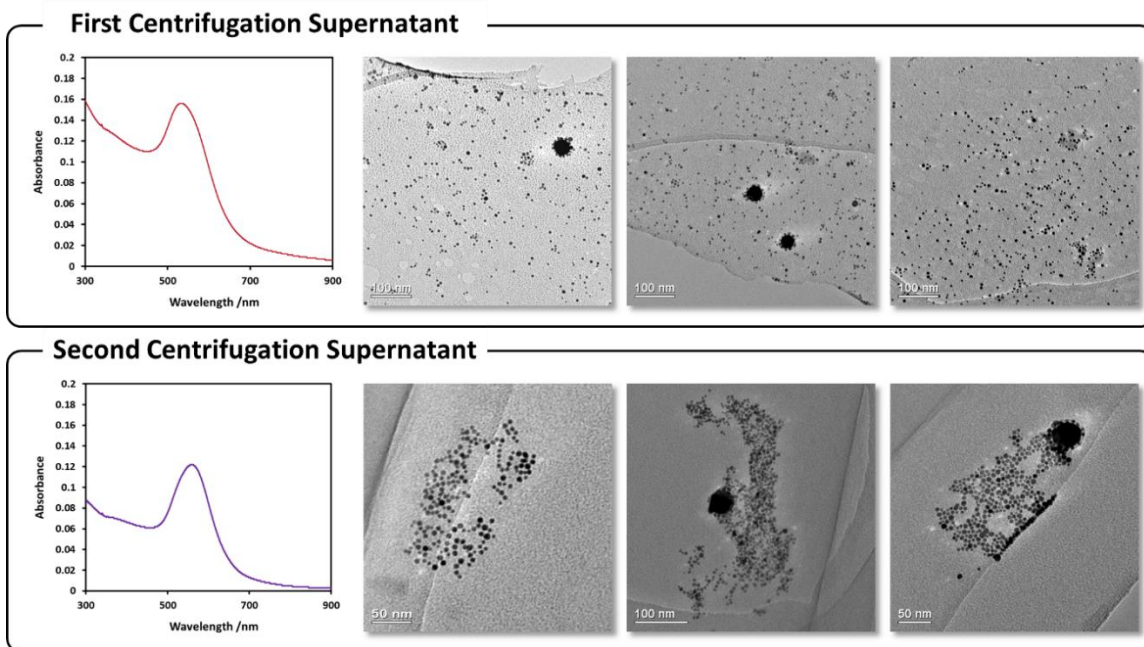


Figure S20 UV-vis spectra (H_2O , 20 °C) and representative TEM images of the supernatant solution removed after centrifugation at each stage of purification. At both stages, very few planet-satellite assemblies were removed, suggesting an efficient purification process.

5.4 Estimation of planet coverage from TEM imaging

It is possible to count the number of satellite NPs on a given planet from TEM images. To account for the fact that TEM produces a two-dimensional image of one side of the assembly, the unseen side must be assumed to be the same as the observed side. For four representative assemblies (Figure S23), taken from images of purified samples, prepared at the optimized ratio of 280:1 (AuNP-1:citrate-NP), satellite coverage has been estimated, revealing a consistent coverage of around 70 satellites per planet. The estimated coverage for samples prepared at higher ratios gave the same result.

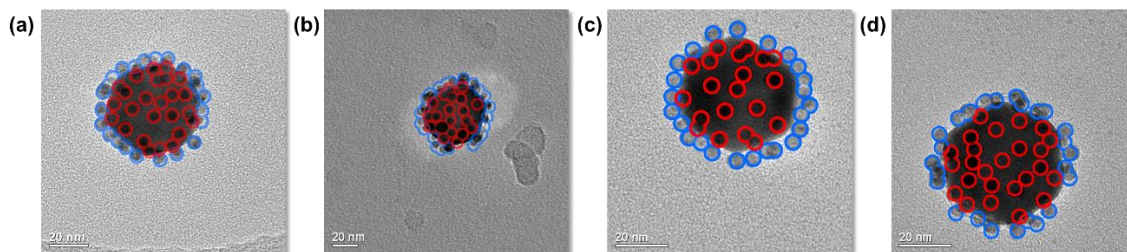


Figure S21 Visualization of satellite NPs on top of the planet is possible by TEM, with all visible satellite NPs highlighted. The edge satellites (blue) and the face satellites (red) were counted to give an indication of the satellite coverage. It is assumed that the unseen face has the same number of satellite NPs on it, therefore, the number of face satellites (red) is doubled. (a) (face: 25; edge: 23) \rightarrow 73 satellites. (b) (face: 20; edge: 23) \rightarrow 63. (c) (face: 20; edge: 24) \rightarrow 64. (d) (face: 25; edge: 25) \rightarrow 75.

5.5 Self-assembly control experiments

Control experiments followed the same procedure as for formation of planet–satellite assemblies, however, with AuNP-1 replaced by AuNP-2 (Figure S26). No assembly formation could be detected either by TEM or UV (Figure S27)

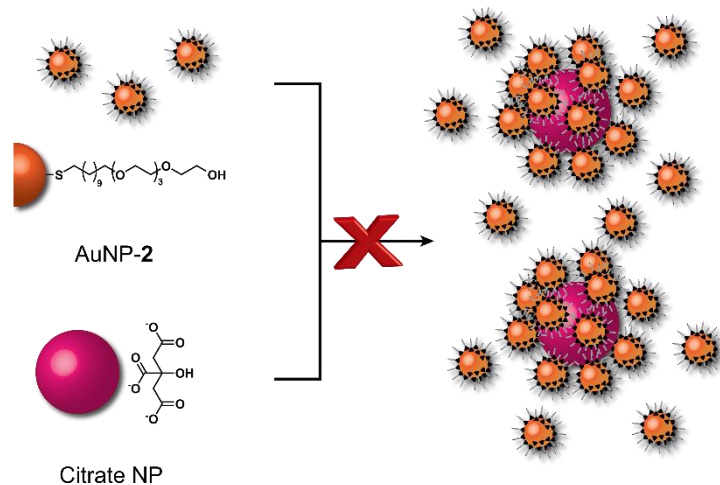


Figure S22 Schematic representation of control experiments using monohydroxy-functionalized AuNP-2.

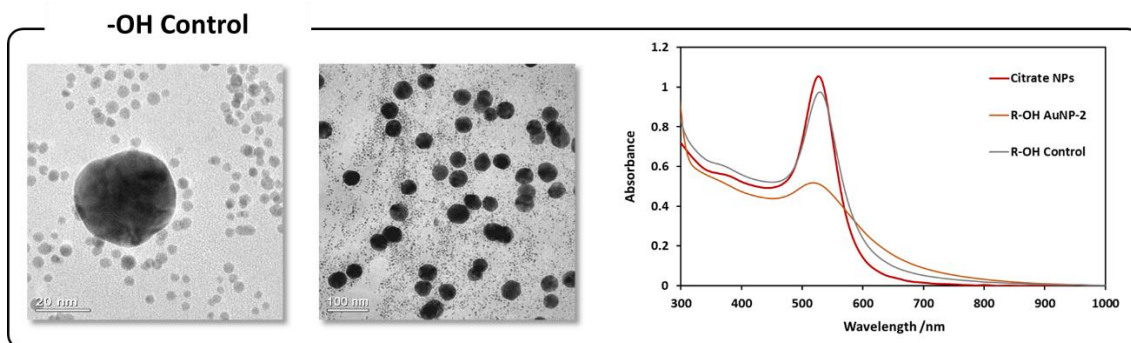


Figure S23 Representative TEM images and UV-vis spectra (H₂O, 20 °C) for control experiments, where hydroxyl-functionalized AuNP-2 was used in place of dihydroxy-functionalized AuNP-1. The TEM images reveal no planet–satellite formation, showing only randomly associated structures formed during the drying process. The absence of aggregates in solution is confirmed by UV-vis analysis, which shows extinction spectra of the mixtures as simple superpositions of the two component spectra, with no shift in the position of the SPR band.

6. Planet–satellite stability studies

6.1 Stability to increased temperature

An aqueous planet–satellite solution (1 mL) was heated to 80 °C for 3 hours. A UV-vis spectrum obtained once the solution had cooled to RT revealed no change from the starting spectrum.

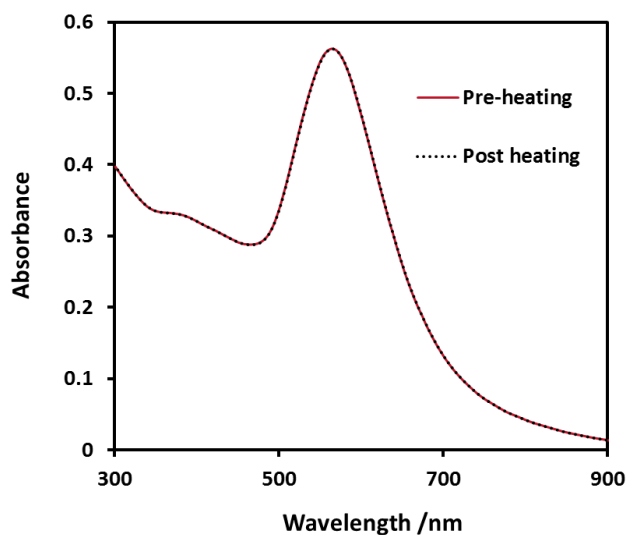


Figure S24 UV-vis spectrum (H₂O, 20 °C) of planet–satellite assemblies prior to and after heating to 80 °C for 3 hours, revealing no change in the spectrum.

In a separate experiment, UV-vis spectra were recorded at 20, 30, 40 and 50 °C. The value of λ_{\max} (SPR) remained unchanged at 564 nm throughout, and the overlaid spectra were found to be indistinguishable.

6.2 Drying and redispersion of planet–satellite assemblies

Redispersion after complete solvent removal

Solvent can be removed from the solution of planet–satellite clusters without disrupting the assembly structure. This may be achieved either by centrifugation (5600 rfc, 5 mins) to induce NP precipitation and subsequent decanting of the supernatant, or by evaporation (either under vacuum or under a stream of air). The assemblies may be redispersed in both cases with no change in the assembly structure.

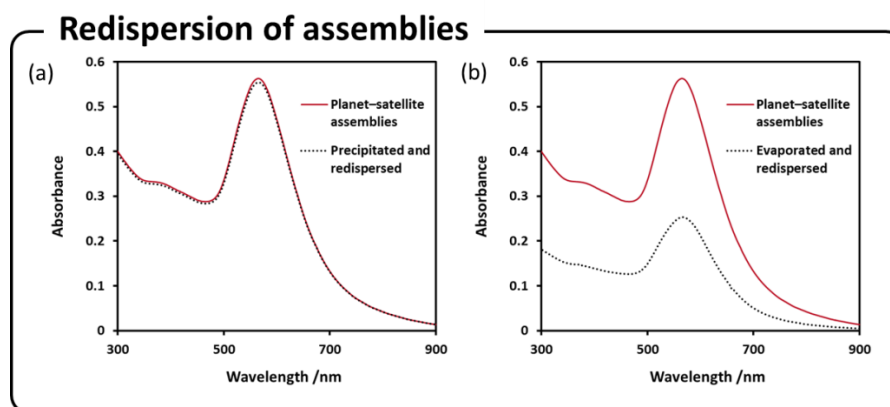


Figure S25 UV-vis spectra (H_2O , 20 °C) of planet–satellite assemblies before solvent removal and after redispersion. (a) Redispersion of planet–satellite assemblies in water after centrifuge-induced (5600 rfc, 5 mins) NP precipitation, and decanting of original solvent. (b) Redispersion of planet–satellite assemblies in water after solvent evaporation under airflow.

Following centrifuge-induced precipitation, the supernatant was carefully removed from the resultant pellet. The pellet remains moist in the process, and was subsequently redispersed in fresh water with no loss of material (Figure S29a).

Following solvent evaporation, redispersion in the same volume of water showed no shift in the SPR band of the assemblies, however a decrease in absorbance is observed (Figure S29b), attributable to irreversible adsorption of assemblies to glass container.

Redispersion in organic solvents

A solution of satellites was centrifuged at 5600 rcf for 5 minutes to induce complete precipitation. Solvent was decanted. Addition of the same volume of MeCN followed by sonication led to complete redispersion of the assemblies.

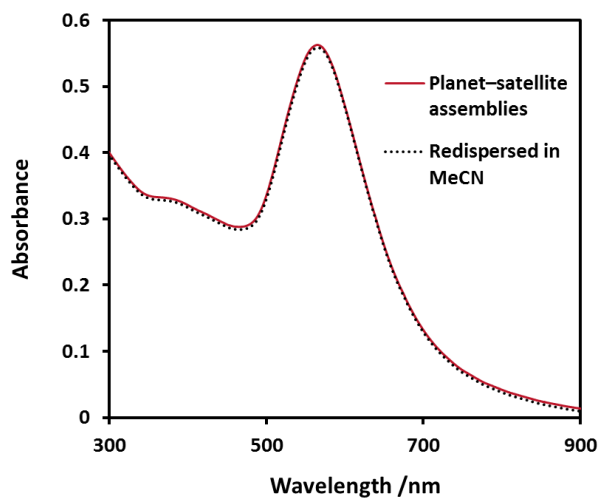


Figure S26 UV-vis spectra (H_2O , 20 °C) of planet-satellite assemblies after redispersion in MeCN.

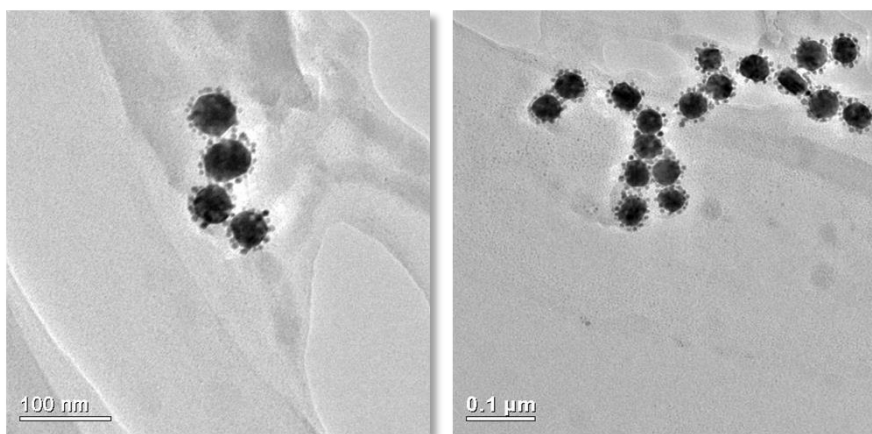


Figure S27 Representative TEM images of planet-satellite assemblies after redispersion in MeCN.

6.3 Stability to increasing ionic strength

Stability to NaCl

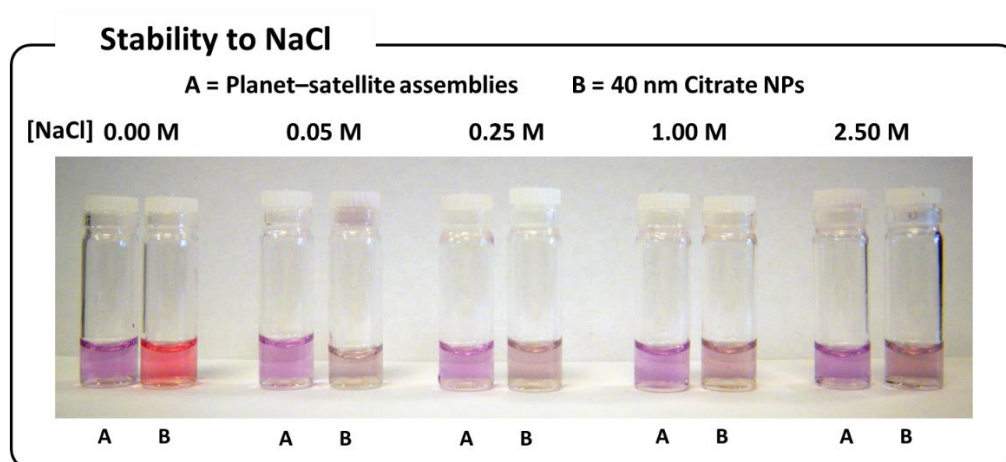


Figure S28 A visual experiment showing the superior stability of the planet-satellite assemblies (A) compared to citrate-stabilized NPs (B) on increasing solution ionic strength. Images were taken 30 minutes after adjusting salt concentrations to the stated values. In all samples up to $[\text{NaCl}] = 2.50 \text{ M}$, planet-satellite assemblies appeared stable, whereas the citrate-NPs were unstable even to low (0.05 M) salt concentrations.

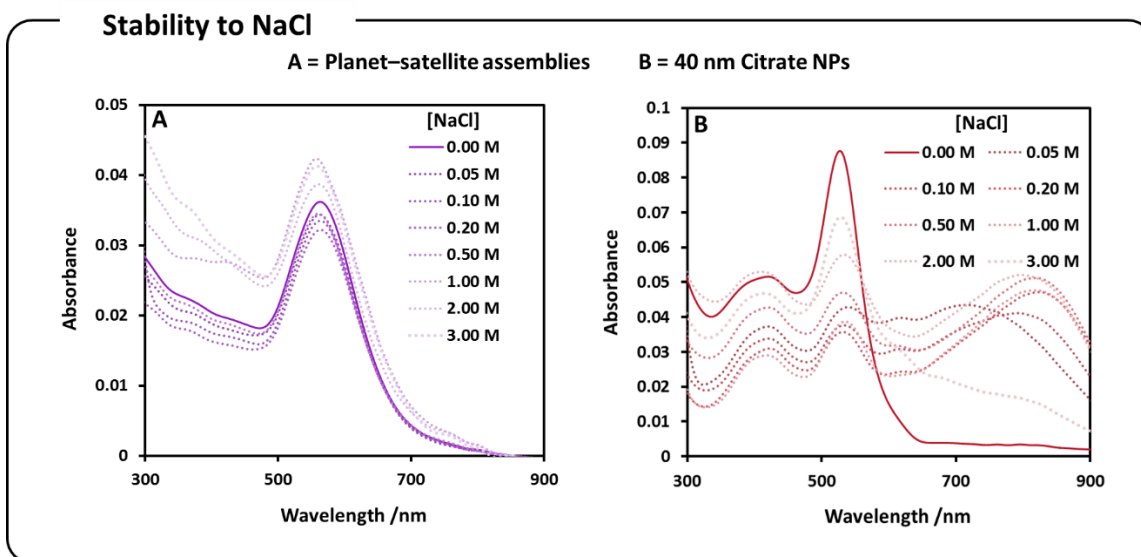


Figure S29 UV-vis spectra (H_2O , $20 \text{ }^\circ\text{C}$) of planet-satellite assemblies (A) and citrate-stabilized NPs (B) in aqueous solution with $[\text{NaCl}]$ ranging from 0.00 M to 3.00 M (all spectra recorded within 3 minutes of addition of NaCl). The planet-satellite assemblies show no change in the position of the SPR band, indicating their stability to high NaCl concentrations (the variation in absolute absorption is not systematic and is attributed to scattering). By comparison, the spectra of citrate stabilized NPs show the emergence of a new peak at 800 nm even at $[\text{NaCl}] = 0.05 \text{ M}$, which blue-shifts as the salt concentration increases, indicating increased aggregation. The disappearance of this peak at very high salt concentrations suggests precipitation of large aggregates from solution.

Stability to MgCl₂

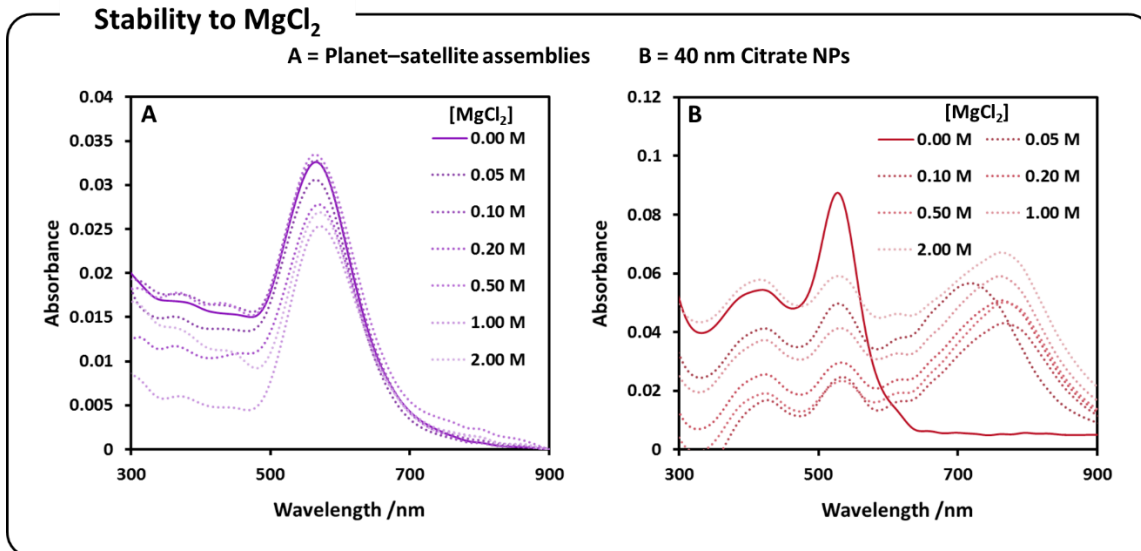


Figure S30 UV-vis spectra (H₂O, 20 °C) of planet-satellite assemblies (A) and citrate-stabilized NPs (B) in aqueous solution with [MgCl₂] ranging from 0.00 M to 2.00 M (all spectra recorded within 3 minutes of addition of MgCl₂). The planet-satellite assemblies show no change in the position of the SPR band, indicating their stability to high MgCl₂ concentrations (the variation in absolute absorption is not systematic and is attributed to scattering). By comparison, the spectra of citrate-stabilized NPs show the emergence of a new peak at 800 nm, even at [MgCl₂] = 0.05 M which blue-shifts as the salt concentration increases, indicating increased aggregation.

6.4 Stability to pH

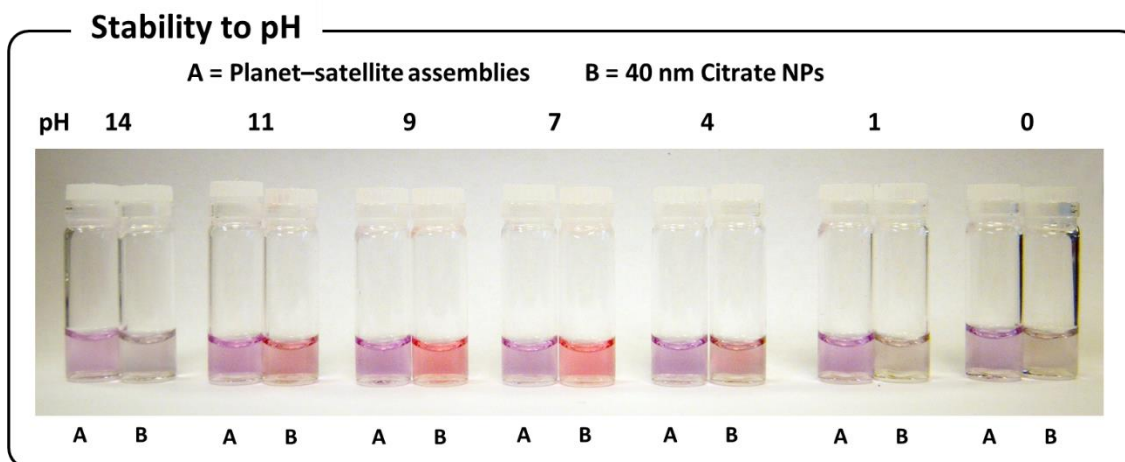


Figure S31 A visual experiment showing the superior stability of the planet-satellite assemblies (A) compared to citrate-stabilized NPs (B) on varying pH. Images were taken 1 hour after adjusting the pH from pH 7 using either HCl or NaOH. Planet-satellite assemblies appeared stable by eye at all pH values. By comparison, the citrate-stabilized NPs were unstable at both low (≤ 4) and very high (≥ 11) pH values. At low values, protonation of the stabilizing citrate layer causes aggregation and precipitation. The instability at high pH values is likely a result of increased solution ionic strength.

7. Scope of planet NPs

7.1 Varying planet NP size

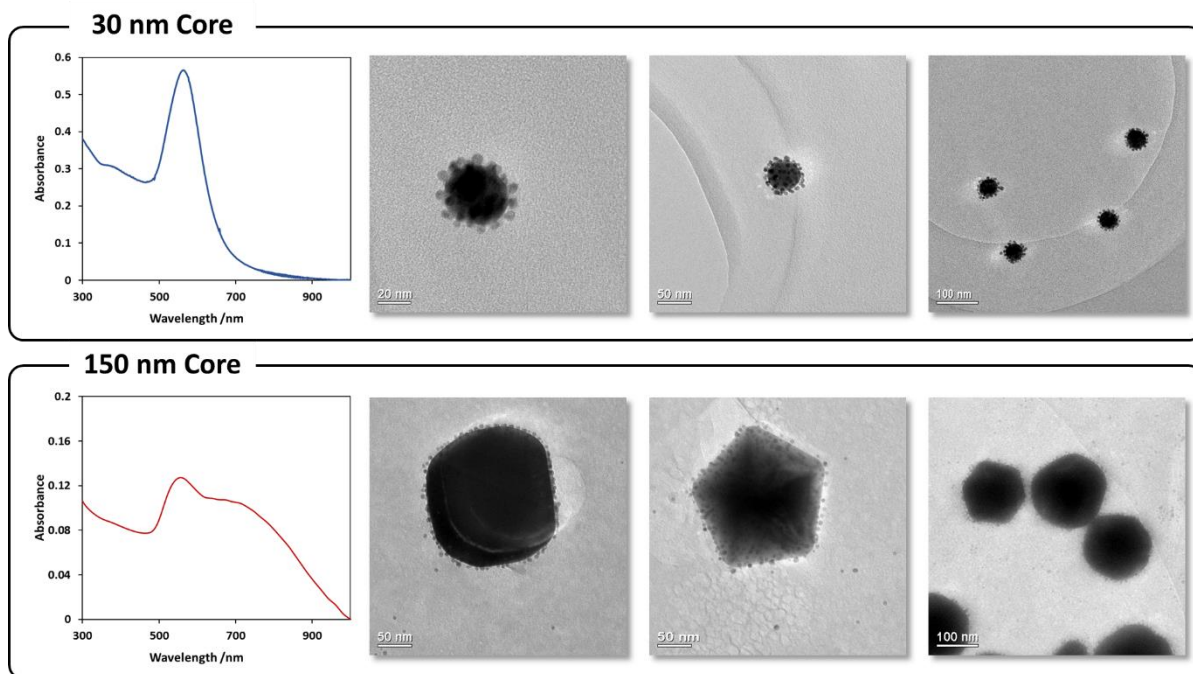


Figure S32 UV-vis (H_2O , 20 °C) and representative TEM images of planet-satellite assemblies with different planet NP sizes: 30 nm and 150 nm. The synthesis and purification procedure was as described for the 40 nm core planet-satellite assemblies.

7.2 Varying planet NP shape

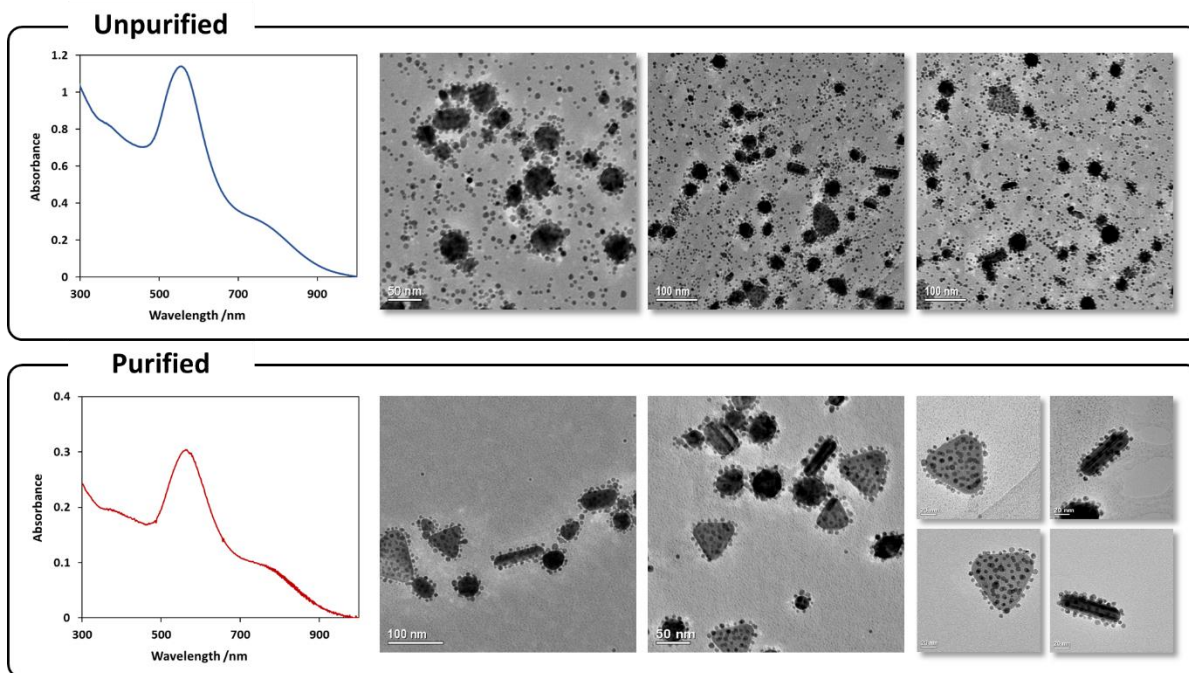


Figure S33 UV-vis (H_2O , 20 °C) and representative TEM images of planet-satellite assemblies with planet NPs of varying shapes and sizes. Synthesis and purification of the sample was carried out as described for the 40 nm planet-satellite assemblies.

8. Varying Satellite NP Size: Preliminary Studies

In order to investigate whether alternative satellite NPs could be employed in the self-assembly process, 10 nm 1,2-dihydroxy alkylthiol stabilized NPs (AuNP-1_10) were prepared by ligand exchange from citrate-stabilized NPs with thiol **1H**, followed by purification by dialysis.

The purified 10 nm AuNP-1_10 were mixed as before with 40 nm commercial citrate-stabilized NPs (0.112 nM, 1 mL) in a 200:1 molar ratio. In contrast to all assembly experiments involving AuNP-1, a colour change was not immediately observed. However, over a period of 24 h, complete precipitation of the colloidal suspension occurred, leaving a colourless supernatant. TEM images of the resulting aggregates clearly show assembly of planet and satellite NPs.

It appears that in this case, precipitation occurs before a complete, stabilizing layer of satellite NPs can form around each planet. Most likely this can be explained by the presence of residual citrate species on the surface of AuNP-1_10. This would result in repulsive electrostatic interactions between satellite NPs and the highly negatively charged planet NPs, as well as between neighbouring satellites. This leads to a more complex set of forces governing NP assembly and colloidal stability, so that stable, complete-shell planet-satellite structures are not produced before kinetically trapped precipitates are formed.

Importantly, a control experiment, where 10 nm citrate-stabilized NPs were mixed with 40 nm citrate-stabilized NPs in the same ratio, showed no colour changes and no precipitation over a period of several days, indicating that the presence of the 1,2-dihydroxy functionality is responsible for NP self-assembly. It should therefore be possible to optimise other routes to 1,2-dihydroxy-stabilized satellite NPs of varying sizes and shapes in the absence of residual charged species, and employ those building blocks in the same self-assembly process. Investigations towards this goal are currently underway in our laboratory.

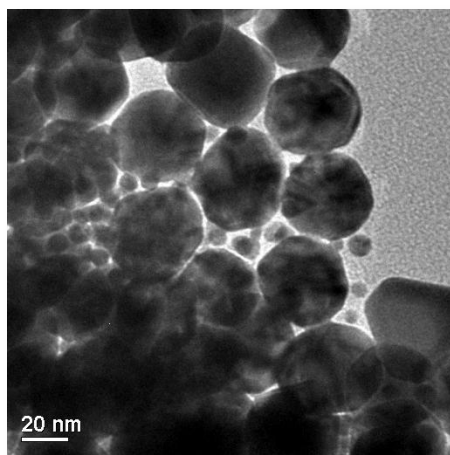
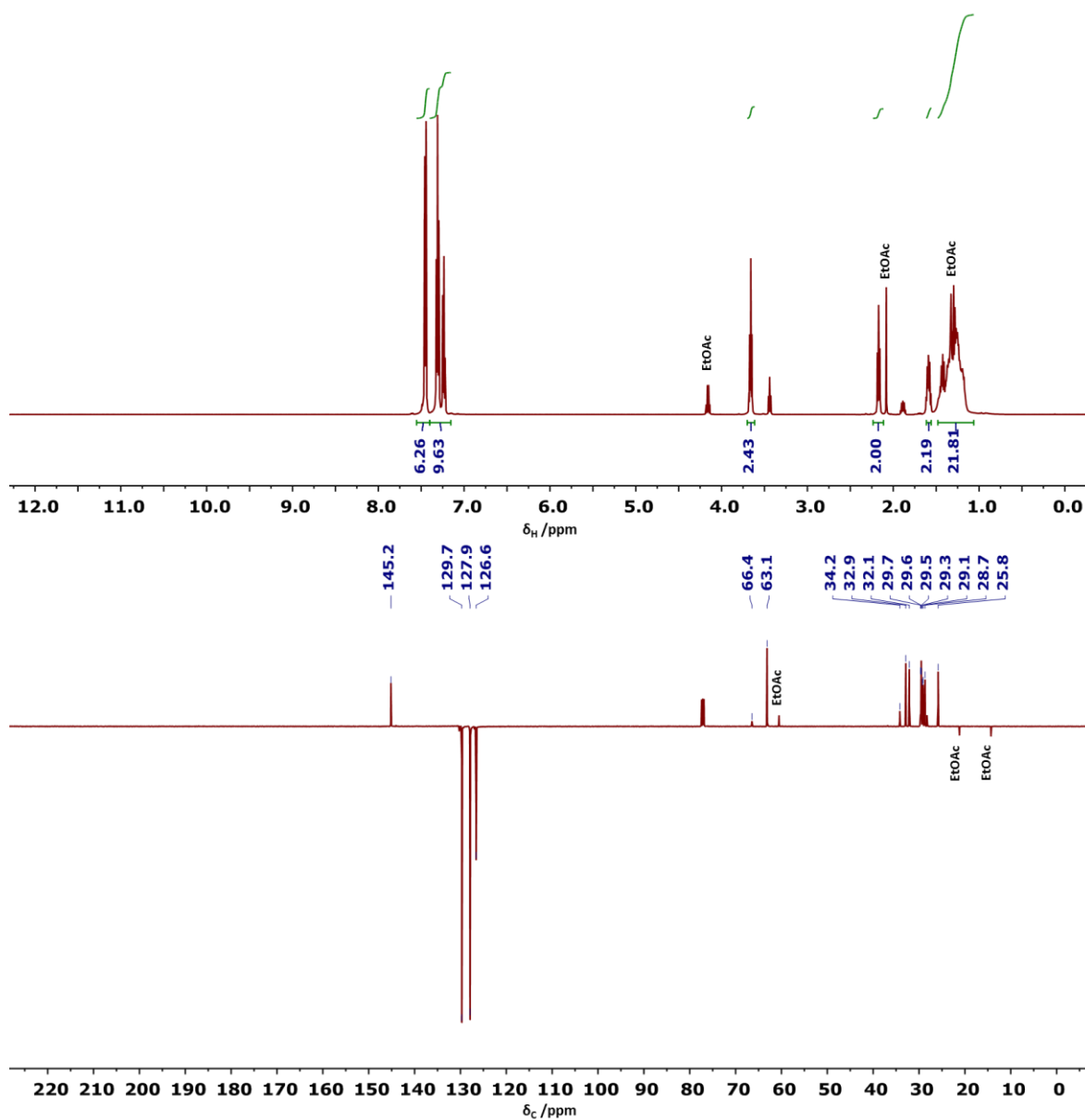
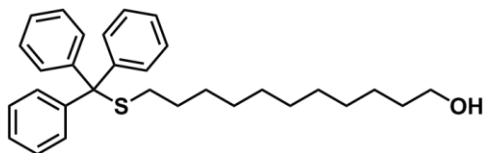


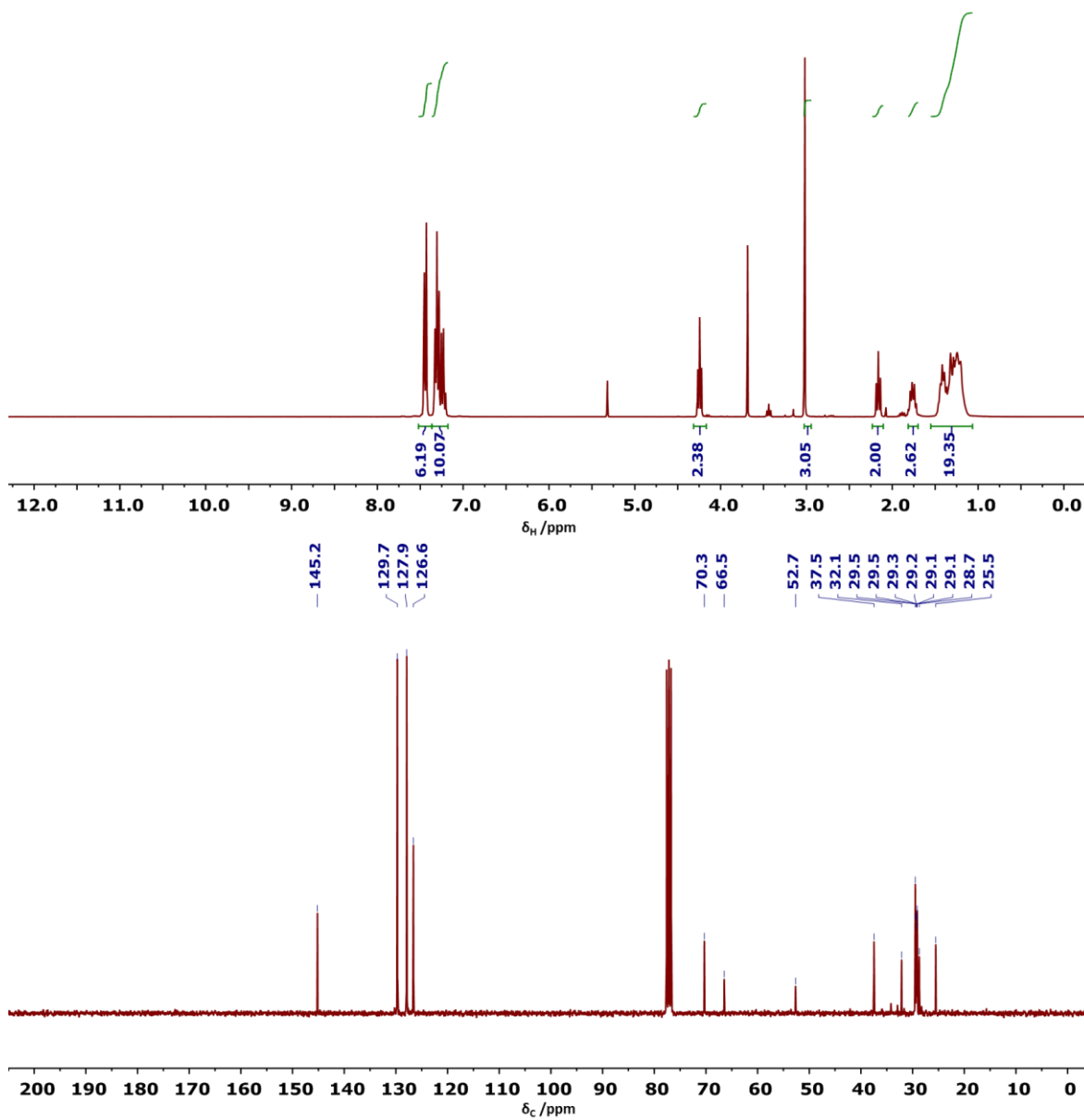
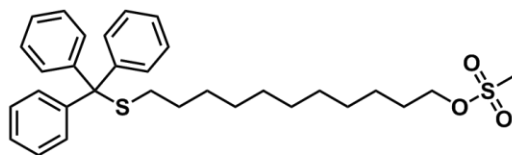
Figure S34 TEM image of AuNP-1_10 mixed with 40 nm citrate-stabilized NPs in a 200:1 molar ratio after 24 hours.

9. ^1H and ^{13}C NMR spectra for organic compounds

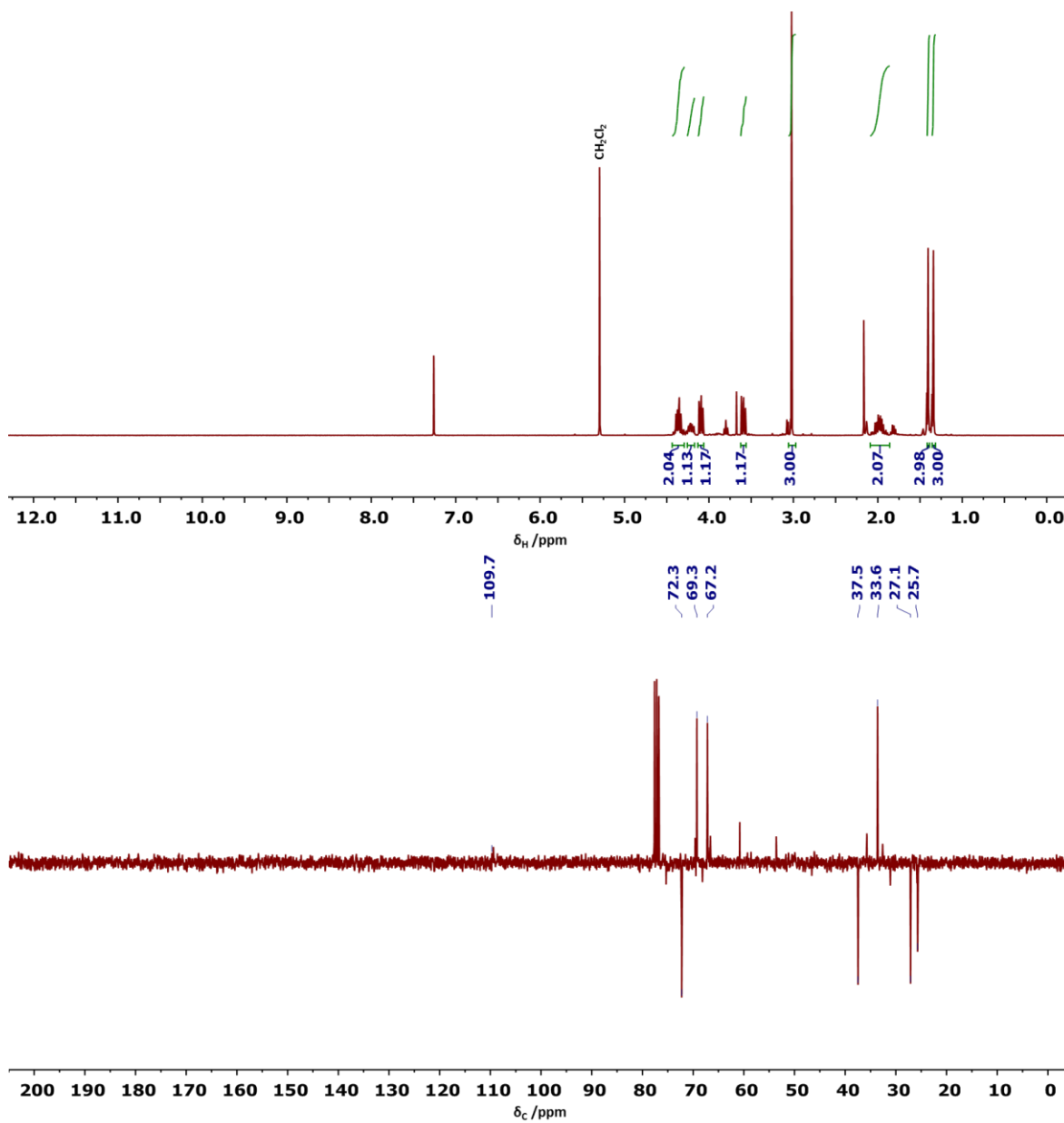
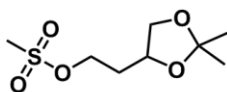
Compound S2: 11-(tritylthio)undecan-1-ol



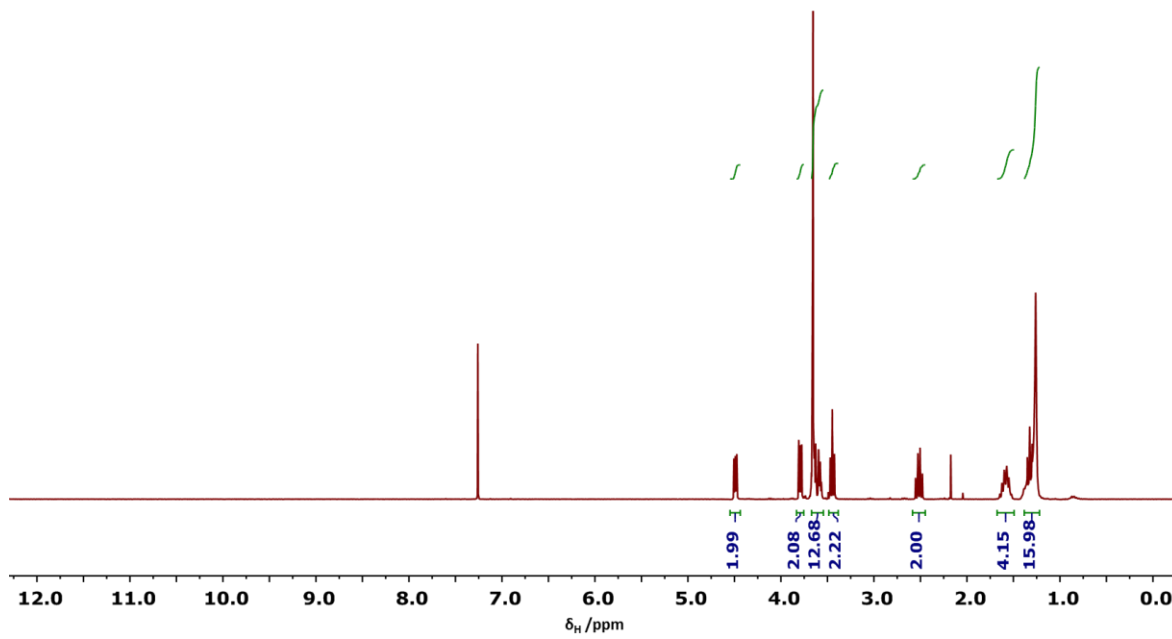
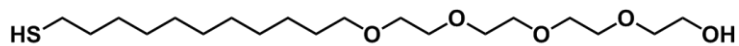
Compound S3: 11-(tritylthio)undecyl methanesulfonate



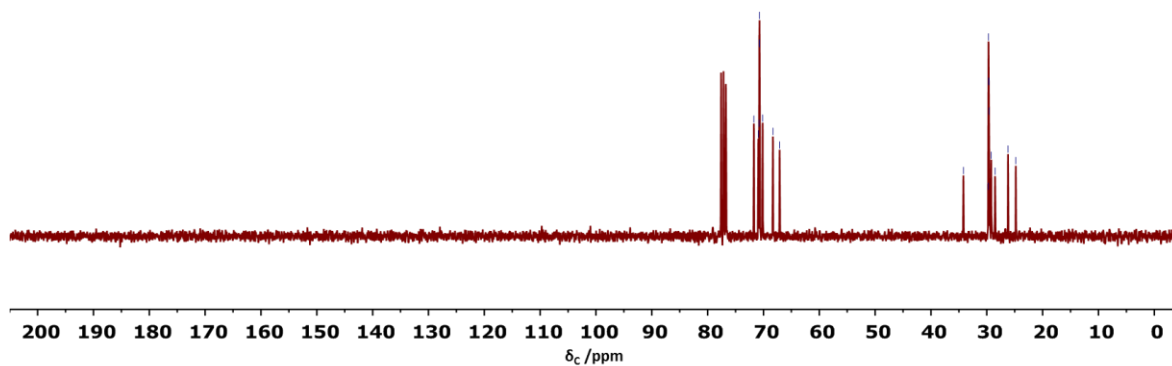
Compound S5: 2-(2,2-dimethyl-1,3-dioxolan-4-yl)ethyl methanesulfonate



Compound 2H: 23-mercapto-3,6,9,12-tetraoxatricosan-1-ol



71.7
70.9
70.8
70.7
70.7
70.7
70.1
70.1
68.3
67.1
34.2
29.7
29.7
29.7
29.6
29.6
29.2
28.5
26.2
24.8



9. References

- [S1] O. R. Miranda, H.-T. Chen, C.-C. You, D. E. Mortenson, X.-C. Yang, U. H. F. Bunz and V. M. Rotello, *J. Am. Chem. Soc.*, 2010, **132**, 5285.
- [S2] H. Perrier, G. Huyer and R. N. Young, *Tetrahedron Lett.*, 1992, **33**, 725.
- [S3] H. Xia, S. Bai, J. Hartmann and D. Wang, *Langmuir*, 2010, **26**, 3585.
- [S4] X. Liu, M. Atwater, J. Wang and Q. Huocoll, *Coll. Surf. B*, 2007, **58**, 3.
- [S5] H. Sellers, A. Ulman, Y. Shnidman and J. E. Eilers, *J. Am. Chem. Soc.*, 1993, **115**, 9389.